Experimental investigation of flammability and numerical study of combustion of shrub of rockrose under severe drought conditions

Frédéric Morandini, P.A. Santoni, J.B. Tramoni, W.E. Mell

Experimental investigation of flammability and numerical study of combustion of shrub of rockrose under severe drought conditions

F. Morandini[a], P.A. Santoni[a], J.B. Tramoni[a], W.E. Mell[b]

[a]Université de Corse CNRS UMR 6134 SPE, Campus Grimaldi, BP 52, 20250 Corte, France

[b]Pacific Wildland Fire Science Laboratory, U.S. Forest Service, 400 N 34th Street, Suite 201, Seattle, WA 98103, USA

Abstract

Structure of vegetation significantly influences its flammability and resulting fire spread. Despite considerable amount of laboratory studies, experimental works carried out with full plant specimens, representative of field conditions, are still limited. Present study aims to collect meaningful experimental data on structure and flammability of shrub of rockrose and evaluate the predictions of a fire model (WFDS) against this dataset. Spatial distribution of fuel elements, sorted according to their characteristic thickness, was established from destructive measurements. 28 fire tests were conducted with full plants under a calorimeter. Foliar moisture content was in the range of 4-18% on dry basis. Radiant panels were used as source of ignition. Flammability was investigated using ignitability, sustainability, combustibility and consumability. Comparison to previous studies highlighted the necessity of standardization among test procedures. Principal component analysis revealed four flammability regimes depending on proportion of thin fuel elements within the crown, position of ignition and duration of preheating. Finally, combustion dynamics of a shrub was numerically investigated with WFDS. A bulk density model was developed from the characterization study and used as input data for the numerical code. Predicted HRR was in good agreement with experiments, although simulation results need improvement in initiation phase of burning.

Keywords: Wildland fires; shrub flammability; Ignitability; Sustainability; Combustibility; Consumability; Mediterranean vegetation; Oxygen Consumption Calorimetry; WFDS.

1. Introduction

Large and severe wildfires have increased in occurrence, duration and intensity the last decade [1]. In 2017, these fires burnt over 1.2 and 4.1 million ha of natural lands in Europe [2] and United States [3], respectively, causing the worst wildfire season on record in many counties across the world. They caused billions of euros in damages and fire suppression costs and killed hundreds of people among fire fighters and civilians. The last catastrophic events that occurred in Portugal in 2017, and in Greece and California in 2018 have sadly confirmed this tendency. Continuous efforts are being made towards the understanding of the behavior of fires at several observation scales (laboratory experiments and field scale observations), the improvement of fire spread models of all types (statistical, semi-empirical, physical or detailed) and the development of decision support tools for fire management.

Vegetation plays a critical role in wildfire spread. Thus, flammability [4-6] of natural fuels is a fundamental aspect to identify potential fire impacts and hazards. It is defined as a combination of four inter-correlated components involving several material and related combustion properties. These components refer to the ability of vegetation to ignite (ignitability), to maintain combustion and produce energy during its thermal degradation (sustainability), to the rate of combustion (combustibility) and to the proportion of biomass consumed (consumability). The first two components of flammability are basically temporal measurements and are easy to evaluate. Thus, ignitability is often defined as the time to ignition [4, 7-9]. Sustainability is usually described as the flame duration [8-11]. The last two components involve combustion metrics and are less straightforward to measure, depending on the technique used. Metrics of various kind, such as flame temperature [8, 12], flame height [9, 12, 13], rate of fire spread [7, 8] or rate of heat release [9, 11] were used as indicator for combustibility. Finally, the consumability has been characterized by the fuel consumption ratio, the residual mass fraction [7, 9, 12] or the mass loss rate [9, 11, 12]. It should be noticed that the whole four components are rarely used together to classify the flammability of natural fuels and ignition properties are often only considered [14, 15].

Flammability is difficult to evaluate since it is not a direct measurable property but a broad concept encompassing several metrics. Unlike for testing building materials, flammability of vegetation can be subject to debate [16] and some authors developed alternative frameworks [17-20]. No standardized procedure exists for evaluating the four components of flammability for natural fuels [9] and different metrics can be used to quantify a same component. For

instance, flame duration (in terms of visual flaming or duration above a threshold of temperature, heat release rate or radiant heat flux), heat of combustion or total heat released or surface area burnt can be used as indicators of sustainability [9]. More questionable is the use of the same metric for the evaluation of different flammability components. In particular, the mass loss rate during combustion was used as descriptor for consumability and combustibility [18, 21], and surface area burnt for sustainability and consumability [9, 18]. Many studies have emphasized the effects of fuel moisture content and fuel geometry on flammability [12, 14, 22-33]. The flammability was also shown to be scale dependent [9, 17, 18, 22, 31, 34]. However, the conditions of the assessment tests are frequently not representative of the ones encountered during wildfires [35]. The flammability tests are usually performed on isolated fuel particles (foliage, needles, litter, twigs, bark…) [14, 15, 33, 36-38] or plant parts (leafy branch) [19, 21, 39, 40] but no relation with the full-plant flammability is provided. White and Zipperer [9] pointed out a lack of good documentation of the behavior of individual plants in natural fires. Indeed, burning characteristics of full-scale plant, characteristic of the field conditions, has received little attention [13, 22, 31, 41-53].

Bench scale calorimeters (cone, fire propagation apparatus, mass loss calorimeter) are usually used to estimate flammability of particular fuel elements or part of plants in the laboratory [22, 33, 37, 39, 54-57]. Such calorimeters have been developed for the study of building materials on a plane surface area basis and some difficulties occur when testing the porous fuel comprising plant parts. Furthermore, the sample holder modifies the back face boundary condition and the air inflow. This can significantly influence the burning behavior of the samples [54-59]. Contrary to micro-scale differential scanning calorimetry (DSC) or thermogravimetric analysis (TGA), where samples are reduced into uniform fine powder solid fuel (losing the link to the structure of the original material), bench scale calorimeters allow to assess the flammability of parts of plant (needles, leaves, twigs) with a heating rate representative of fire conditions in the open. However, the manual arrangement of the samples of vegetation used for fire tests at bench scale (litters, plant parts) alters the structure of these natural fuels. Indeed, the reconstruction of the vegetation layer modifies both its compactness and bulk density [60]. These changes influence ventilation within the fuel layer and resulting fire behavior [61, 62]. Consequently, the relationship between bench scale results on plant parts and flammability of the whole plant still needs to be addressed, making even more difficult to extend these tests to field fire scenarios.

The plant geometry, structure and composition (leaves, twigs of various diameters) were already identified as primary parameters determining its flammability [16, 35, 63-66]. Experimental studies have also shown the effects of the size and spacing of fuel elements during fire tests [47, 66-70]. The particles of various kind and size, that compose the vegetation, participate in different ways in the combustion mechanisms that occur during fire spread. Typically, only fuel elements smaller than 6 mm in diameter contribute to the fire behavior [71]. The thinner the particles, the sooner they are involved in the thermal degradation processes [11, 36, 38]. Indeed, the leaves, needles or twigs (thickness ≤ 2 mm) are very prone to heating via convective heating and direct flame contact [72]. An increase in the proportion of overall fuel mass that is thin fuel elements was shown to result in the increase of both energy content [13] and proportion of fuel burnt [73].

Considering the difficulties with establishing relationships between heat release for the individual parts and the whole plant, the use of calorimetry measurements at full-scale seems a suitable alternative [9]. Few studies [13, 22, 31, 41-51, 53] were conducted to measure the burning characteristics for whole plants. The majority focused on some specific components of the flammability. The measurements of the burning characteristics performed on full scale plants are synthetized in Table 1 and are expressed in relation to flammability components. Some of these studies used calorimetry to provide the measurement of the Heat Release Rate (HRR) which is among the most important parameters for understanding flammability, characterizing fire hazard and ranking fuels [74]. This fundamental property can also be used to estimate potential for ignition of adjacent fuel elements along with emitted radiant heat flux. The main difference between fire tests carried out at bench scale and full scale is that the natural structure of the vegetation is kept intact in the latter. Furthermore, the flame spread across the whole plant is taken into account [20, 44]. The comparison of results collected at different scales is a complex task [11]. Experiments carried out on the same fuels at different scales showed contradictory conclusions. While some authors measured a reasonable agreement between both scales [75] others obtained either an increase of peak HRR with increasing scale [22] or the opposite outcome [11, 59]. Moreover, considering the wide range of sample conditioning (fuel elements, parts of plants, full-scale plants), ignition method (radiant source, flame) and fire test conditions (still air or wind to favor combustion), the evaluation of the flammability components is highly dependent of the experimental procedure. As a result, differences in fire behavior can be related to the experimental setup rather than vegetation characteristics.

Fire experiments were reported to offer a limited insight into vegetation-fire dynamics interactions and physics-based fire spread models were suggested to be the best way for understanding plant flammability [35]. Numerical simulations, based on computational fluid dynamics [30, 76-83], have been extensively used to improve the knowledge of fire spread across vegetation at various scales and could have practical applications in fire and landscape managements. These models need to be compared over a wide range of configurations for sub-models improvement purposes. In particular, the Wildland-urban interface Fire Dynamics Simulator (WFDS) was tested at field scale with large experimental grassland fires [83]. However, this first modelling approach considered only a boundary fuel model. Next, the spatial distribution of different fuel elements (leaves, twigs) within a vegetation layer was implemented [80], but char combustion processes was nevertheless not considered at this stage. Further improvements have consisted in the modification of the thermal degradation sub-model in order to include the char oxidation, the refinement of the gasification law [79]. The predictions were in a satisfactory agreement with the experimental data on fire spread across pine needle beds.

The present study focusses on the experimental and numerical investigations of the flammability of single shrubs of rockrose. The first aim is to characterize the distribution of the fuel elements (leaves and twigs of various diameters ranked by size classes) within the shrub. From these experimental data, the distribution of each class of particles is estimated. The resulting bulk density is then used as input for WFDS. The second aim is to assess the shrub flammability based on the four components (ignitability, sustainability, combustibility and consumability). The fire tests were conducted with dried shrubs with unmodified structure submitted to an external heat flux (radiation alone), providing a flammability measurement much closer to that of individuals in the field than those obtained from parts of plants. An originality of the work lies in the measurements of HRR (by oxygen consumption calorimetry) and fuel consumption at particle level (from destructive sampling of burned shrubs) as indicators of the shrub combustibility and consumability, respectively. The predictions of WFDS are then evaluated against this dataset in order to test this model and highlight future improvement directions.

2. Material and Methods

2.1.Vegetation characterization

Accurate vegetation characterization is required to assess the flammability of complex fuel such as shrub. The present work focuses on shrubs of rockrose (C*istus monspeliensis*), an abundant vegetation of the Mediterranean basin, typical of maquis, that is frequently involved in wildland fires. This pyrophytic species is known for his level of invasiveness in these areas, particularly in Corsica where the study is conducted. Furthermore, the shrub of rockrose has a large seasonal variability of moisture content of live fine fuel [32]. Consequently, it is difficult to eliminate outside of the fire season using prescribed burnings since they are conducted under very high foliar moisture content conditions (>200%) that result in marginal burning. Paradoxically during summer, it generates high intensity fires, hard to suppress and often responsible of firefighters fatalities in steep slope and wind conditions [84, 85]. Indeed, for small shrubs, moisture content can decrease during this season down to values lower than 20% [86] and thus these plants reach an even higher fire hazard when period of intense droughts occurs. The shrub of rockrose is composed of fuel elements of different size distributed non uniformly. From top to bottom the shrub is composed of a crown containing leaves and small twigs, an intermediate part mainly formed of twigs of several diameters and a base made of largest fuel elements. As a first step toward a better understanding of the fire spread mechanisms across shrublands, a characterization study of the shrubs of rockrose was performed. Measurements of the shrub structure (proportion and 3D spatial distribution of fuel particles of different kind and size) were carried out on three shrubs harvested in central region of Corsica, France (42°17'N, 9°10'E) during autumn. The base of the rockroses composed of large fuel elements was not considered in this study. Such large diameter twigs (>25 mm in diameter) don't participate in the dynamics of fire spread although they could be thermally degraded and burned after long exposure within the fire front, depending on fire intensity. The plants were harvested in the same vegetation plot and were chosen to be approximately the same size and relatively uniform in shape. They were cut off a few centimeters above the ground. The average (± standard deviation) height of the samples of rockrose was 1.23 ± 0.12 m. The average crown depth and diameter (measured at mid-crown height) were 0.35 ± 0.07 m and 0.68 ± 0.06 m, respectively. The overall shrub mass (excluding the bottom of the base attached to the roots), on live and dry basis, were 1.30 ± 0.28 kg and 0.76 ± 0.03 kg, respectively. In order to determine qualitatively and quantitatively the different fuel elements constituting this shrub species, a sampling was performed at particle level according to the cube method [15, 87, 88], which

allows determining the structure of the plant. To this end, each shrub of rockrose was placed within a 1.45 m high, 0.9 m long and 0.9 m wide metallic frame spatially divided into 252 small cubes with sides of 15 cm. The position of each cube was indexed following its 3D (x, y, z) position. All the vegetation contained in these cubes was cut and oven dried at 60°C for 48 hours. Finally, for each cube, the vegetation elements were sorted according to the six size classes (leaves, dead twigs with 0-2 mm diameter, live twigs with 0-2 mm, 2-4 mm, 4-6 mm and 6-25 mm diameters, respectively) and weighed. Thus, both live and dead fuel particles were considered. Unfortunately, this process is destructive and the characterized samples could not be used for the combustion study.

2.2. Flammability experiments

A series of 28 fire tests was conducted with unmodified shrubs of rockrose. The plants were harvested within the same vegetation plot that the ones used in the characterization study described above during several seasons (spring, summer and autumn). Shrubs were cut at their base and stored carefully in a room in order to preserve as well as possible their original structure. Their dimensions and weight are provided in Table 2. The average height of the shrub samples, h_{shrub} was 1.25 ± 0.12 m. The average crown height and diameter were 0.3 ± 0.1 m and 0.7 ± 0.1 m, respectively. The overall mass of the shrubs was 1.95 ± 0.47 kg on wet basis. The initial foliar moisture content (MC) of the fresh sampled shrubs was greater than 100% of the dry weight. Preliminary tests exhibited that, after ignition, the sustained combustion of shrubs with MC greater than 25% failed and their crown was not fully consumed. Furthermore, Terrei et al. [21] indicated that fire spread simulation using WFDS, at the scale of a branch, was possible if the fuel moisture content remained lower than 25%. The present study, combining experimental and numerical investigations, was thus restricted to shrubs with low MC representative of severe drought conditions [25] leading to high fire risk. The plants were air-dried during at least 48 hours in a room with an ambient air temperature of about 25°C and a relative air humidity of about 50 %. This conditioning process resulted in a foliar MC in the range of 4-18%, suitable for the combustion of the full shrub crown. About 10 g sub-samples of twigs < 2 mm in diameter with their leaves were taken from each shrub sample to determine their MC at the time of burning. These sub-samples were oven-dried at 60°C for 48 h and weighted.

A large-scale calorimeter was used to assess the flammability of full-scale shrubs of rockrose. Combustion took place under a 3 m × 3 m hood with a 1 $m^3.s^{-1}$ flow rate extraction

system that handled the combustion products. With this device, the HRR during the combustion of vegetation samples can be measured from oxygen consumption. The details of the technique are provided in the next section and a layout of the experimental setup is provided in Fig. 1. The shrubs with a structure kept almost intact compared to field conditions were mounted on a cylindrical sample holder located on a 3 g precision load cell with full-scale capacity of 15 kg. The balance has a voltage output for external recording of the biomass loss versus time during thermal degradation. The measurements sampling rate was 1 Hz. A moving average method over a 5 s-period, was used to smooth the mass recordings and estimate the mass loss rate (MLR). Four 0.5 m × 0.5 m radiant panels were used to preheat and ignite the vegetation samples. In order to maximize the radiation impinging on the shrub samples, two sets of two radiant panels were used in a corner configuration in order to concentrate the emitted heat flux. The shrub samples were positioned 2 centimeters from the radiant panels in order to avoid direct contact which could led to instantaneous ignition of the leaves located in this region. The maximum temperature of the radiant panels was 520°C, leading to a radiant heat flux of 20 $kW.m^{-2}$ impinging the nearest leaves and twigs of the shrub. Despite a lesser thermal exposure, the electrical heaters were preferred over propane fed radiant panels, because of their fluctuating properties. Indeed these burners induce a bias difficult to compensate during the HRR measurement of burning shrubs. The radiant panels were left on throughout the whole experiment to allow the shrub sample to be preheated. No pilot flame or spark igniter were used and combustion was initiated by auto ignition. Video recordings were applied to monitor the fire growth across the shrub. Unfortunately, flame from burning shrubs was frequently in contact with the extraction hood, and no useful information could be obtained from the measurement of the flame height. The metrics retained for the characterization of each flammability component is provided in Table 1 and compared to previous literature studies. The time to ignition (TTI) and flame duration (FD) were recorded for each fire test to measure ignitability and sustainability, respectively. Consumability was evaluated from the fuel consumption ratio (FCR) at both the particle level, η_k, and in total, η, defined respectively by the following equations:

$$\eta_k = 1 - \frac{m^r_{k,dry}}{m_{k,dry}} \quad (1)$$

$$\eta = 1 - \frac{m^r_{dry}}{m_{dry}} \quad (2)$$

where $m_{k,dry}$ and $m^r_{k,dry}$ represent respectively the initial and residual masses of the *k*-class of particles on dry basis. m_{dry} and m^r_{dry} are the initial and residual masses of the shrub, respectively, on dry basis. In order to assess $m^r_{k,dry}$ as a fine indicator of consumability the vegetation characterization method (described in the previous section) was performed on burnt samples. The assessment of the variable characterizing the last flammability component (combustibility) is described in the next section.

2.3. Heat release rate measurements

The 1 MW Large Scale Heat Release apparatus (LSHR) used to assess HRR was manufactured and calibrated by Fire Testing Technology Limited (FTT). Probes for gas sampling and exhaust flow rate measurement, along with laser smoke measurement, are contained in a 0.4 m inner diameter duct insert. The measurement of the HRR is crucial for understanding the combustion processes and assessing the flammability of materials, more particularly for the study of full-scale plants with complex structure. The combustibility of the samples was assessed using quantities derived from the HRR time history, namely the growth rate and peak HRR. The growth rate was used because during the early period of the fire tests the experimental data supported that the fires grow according to a square law, like most flaming fires [89, 90]:

$$HRR = \alpha\, t^2 \quad (3)$$

where α and t are the fire growth parameter ($kW.s^{-2}$) and the time from ignition (s), respectively.

As for many natural fuels, the combustion of shrub of rockrose can be represented by a reaction of the complete combustion of lignocellulosic materials. As the experiments were conducted under well-ventilated conditions, a stoichiometric reaction can be assumed for the combustion of shrub of rockrose:

$$C_{4.04}H_{5.81}O_{2.76} + 4.11\,(O_2 + 3.76\,N_2) \rightarrow 4.04\,CO_2 + 2.90\,H_2O + 15.46\,N_2 \quad (4)$$

The HRR is estimated from oxygen consumption [91, 92] assuming a constant amount of energy released per unit mass of oxygen consumed, E:

$$\mathrm{HRR} = E\left(\dot{n}^{\circ}_{O_2} - \dot{n}_{O_2}\right)W_{O_2} \quad (5)$$

where W_{O_2} is the molecular weight of oxygen, $\dot{n}^{\circ}_{O_2}$ and $\dot{n}_{O_2}$ are the molar flow rates of O_2 in incoming air and in the exhaust duct, respectively. A more accurate estimation than the standard

value of the energy constant (based on average of many fuels) was determined from the fuel ultimate analysis and low heat of combustion resulting in a value of E = 14.32 *MJ/kg* of O_2 for natural fuels.

In order to assess the HRR, the primary measurements are the oxygen and carbon dioxide concentrations and the exhaust flow rate. The LSHR is an open combustion system in which the incoming air is assumed to be a mixture composed of oxygen (20.95%), carbon dioxide, water vapour and nitrogen. During fire tests, the exhaust gases were sampled within the duct insert at a flow rate of about 3.5 $L.min^{-1}$. Gas measurements were performed using O_2/CO_2 analysers developed specifically for FTT calorimeters, incorporating an enhanced Servomex 4100 featuring a high stability temperature controlled paramagnetic oxygen sensor with flow control and by-pass for fast response time. The response time of the measurements of the oxygen and carbon dioxide concentrations were 11 and 8 s, respectively. Water vapour was removed from the sample gas before analysis of gas concentrations . A two-step drying process was achieved by passing the gas sample consecutively through a cold trap and drying column containing desiccant agent (Drierite). The exhaust flow rate was estimated using bi-directional probe and thermocouple measurement. Accuracy was improved by the use of a differential pressure transducer adapted to the range of flow rates.

The calculations of the HRR and associated parameters were automatically performed using gas concentrations (O_2 depletion and CO_2 correction), exhaust flow rate and analysers response times, based on the three following relations [91, 92]:

$$HRR = \frac{E\rho_0 W_{O_2}}{W_{air}}\left(1 - X^{\circ}_{H_2O}\right)X^{\circ}_{O_2}\dot{V}_{s,298}\left[\frac{\phi}{(1-\phi)+\alpha.\phi}\right] \tag{6}$$

$$\dot{V}_{s,298} = 22.4A\frac{k_t}{k_p}\sqrt{\frac{\Delta P}{T_S}} \tag{7}$$

$$\phi = \frac{X^{\circ}_{O_2}\left(1 - X_{CO_2}\right) - X_{O_2}\left(1 - X^{\circ}_{CO_2}\right)}{X^{\circ}_{O_2}\left(1 - X_{CO_2} - X_{O_2}\right)} \tag{8}$$

where X°_i and X_i denotes the measured mole fraction of species i in the incoming air and exhaust gases, respectively, ρ_0 is the density of dry air at 298 K and 1 *atm.*, W_{O_2} and W_{air} are the molecular weight of O_2 and air, respectively, A is the cross sectional area of the duct, k_t is a constant determined via a propane burner calibration, k_p=1.108 for a bi-directional probe, ΔP

is the pressure drop across the bi-directional probe and T_s is the gas temperature in the duct. $\dot{V}_{s,298}$ and ϕ are the standard flow rate in the exhaust duct measured in the duct insert and the expansion factor for the fraction of the air that was depleted of its oxygen, respectively.

2.4.Data analysis

In order to highlight the main trends observed through the flammability and shrub variables, relationships were sought using simple linear regression (least square fitting). The equation of the linear fits and 95% confidence intervals are provided (determination coefficient and p-value are also given). Analyses were performed using R software (ver. 4.3.2, R Project for Statistical Computing).

Principal Component Analysis (PCA) was performed to investigate the clusters from the various flammability components and related variables, particularly among combustibility and consumability for which different regimes were observed. The previously defined component metrics were used as input parameters for the statistical analysis of global flammability. Analyses were performed using Minitab software (ver. 17.1.0, Minitab LLC).

2.5.Numerical study

The Wildland-urban interface Fire Dynamics Simulator (WFDS, ver. 6.0.0) is a physical model developed by the U.S. Forest Service. It is an extension of the National Institute of Standards and Technology's structural Fire Dynamics Simulator (FDS) to forest fuels. The model is based on coupled equations governing heat and mass transfers between solid and gas phases. Large-Eddy Simulation (LES) numerical method is used to solve the conservation equations of momentum, mass and energy in the gas phase. Full details of the modeling approach are provided in [79, 80]. For the present study, the gas phase model was left untouched, the radiative fraction was estimated to be 27%, from the methodology proposed in [93]. As far as the solid phase is concerned, the thermal degradation models for the desiccation, pyrolysis and char oxidation processes are based on Arrhenius laws [79, 80]. In the condensed phase model, the bulk density $\rho_{b,k}$ and specific heat $c_{p,k}$ for each particle class have contributions from dry fuel, moisture content, char and ash. The solid phase equations for a *k*-class of particles, considered as thermally thin, are given by:

$$\frac{d\rho_{bk}}{dt} = -R_{k,H_2O} - (1-\chi_{char})R_{k,pyr} - (1-\chi_{ash})R_{k,char} \quad (9)$$

where $\chi_{char} = 0.27$ is the mass fraction of dry vegetation converted to char and $\chi_{ash} = 0.13$ represents the fraction of char converted to ash. The Arrhenius rate equations for drying, pyrolysis, and char oxidation are

$$R_{k,H_2O} = \rho_{bk,H_2O} A_{H_2O} T^{-\frac{1}{2}} e^{-\frac{E_{H_2O}}{T_k}} \quad (10)$$

$$R_{k,pyr} = \rho_{bk,dry} A_{pyr} e^{-\frac{E_{pyr}}{T_k}} \quad (11)$$

$$R_{k,char} = \frac{A_{char}}{\nu_{O_2,char}} \rho_g Y_{O_2} \sigma_k \beta_k e^{-\frac{E_{char}}{T_k}} (1 + \beta_{char}\sqrt{Re_k}) \quad (12)$$

where the values of the kinetic constants for drying, pyrolysis and char oxidation are $A_{H_2O} = 600000\ K^{\frac{1}{2}}.s^{-1}$, $A_{pyr} = 39929\ K^{\frac{1}{2}}.s^{-1}$ and $A_{char} = 193.5\ K^{\frac{1}{2}}.s^{-1}$, respectively. The corresponding activation energies are $E_{H_2O} = 6262$ K, $E_{pyr} = 7389$ K and $E_{char} = 8191$ K, respectively. The value of these parameters was optimized (varied at maximum of 10% compared to previous study on pine needle beds [79]) in order to best fit the HHR curve for shrub of rockrose. Re_k represents the Reynolds number, $Re_k = \frac{2\rho_g |u| r_k}{\mu}$ with $r_k = \frac{2}{\sigma_k}$, σ_k and β_k are the surface to volume ratio and compactness of the *k*-class of particles, respectively.

$$\rho_{bk} c_{pk} \frac{dT_k}{dt} = -\Delta h_{vap} R_{k,H_2O} - \Delta h_{pyr} R_{k,pyr} - \alpha_{char} \Delta h_{char} R_{k,char} + Q_k \quad (13)$$

with

$$Q_k = -\langle \dot{q}'''_{c,k} \rangle_{V_b} - \langle \nabla . \dot{q}''_{r,k} \rangle_{V_b} \quad (14)$$

where T_k is the temperature of the *k*-class of particles. The first three terms of the right-hand-side of eq. (13) represent endothermic drying, endothermic pyrolysis and exothermic char oxidation, respectively. The non-dimensional weighting parameters, α_{char}, is the fraction of the heat generated by the char oxidation which is absorbed by the solid fuel element and is empirically set to 0.5 [76]. The resulting fraction of the heat transferred to the gas phase is thus $(1 - \alpha_{char})$. The heats of reaction for evaporation, pyrolysis and char oxidation are $\Delta h_{vap} = 2259$ kJ.kg^{-1}, $\Delta h_{pyr} = 418$ kJ.kg^{-1} and $\Delta h_{char} = -32740$ kJ.kg^{-1}, respectively. The terms in the

right hand side of eq. (14) are the fuel element bulk contributions of convective and radiative heat transfer, respectively.

3. Results and discussion

3.1. Vegetation characterization

A detailed characterization of 3 shrubs of rockrose was firstly performed in autumn paying a particular attention to the fuel elements composing it. The particles were divided into the following classes: leaves, 0-2 mm, 2-4 mm, 4-6 mm and 6-25 mm diameter twigs. Their surface area-to-volume ratio (σ) was 2081, 1733, 1000, 666 and 400 m^{-1}, respectively. The density (ρ) of leaves and twigs was 478 and 961 $kg.m^{-3}$, respectively. The following data are presented on dry basis as a function of non-dimensional height $z^* = \frac{z}{h_{shrub}}$, where z and h_{shrub} are the sampling height and shrub height, respectively. The mass distribution, $\zeta_{k,dry}(z^*)$ and mass fraction, $\gamma_{k,dry}(z^*)$, of a *k*-class of particles, were calculated as follows:

$$\zeta_{k,dry}(z^*) = \frac{m_{k,dry}(z^*)}{\sum_{z^*} m_{k,dry}(z^*)} \quad (15)$$

$$\gamma_{k,dry}(z^*) = \frac{m_{k,dry}(z^*)}{\sum_{k} m_{k,dry}(z^*)} \quad (16)$$

where $m_{k,dry}$ represents the mass of the *k*-class of particles on dry basis.

The mass distribution (Fig. 2.a) shows how particles of a *k*-class are distributed within the shrub. The thin particles (leaves and live twigs ≤ 2 mm in diameter) are mainly located for z^* in the range of 0.77-1.00. It should be noted that they represent 35.0 ± 0.4 % of the total mass of the shrub of rockrose. The Fig. 2.b displays the predominance of a class of particles over the others for a given height. As an example, large fuel elements (twigs > 4 mm in diameter) are predominant for z^* in the range of 0.00-0.46. The analysis of these results allows the delimitation of three zones: the crown composed of thin particles (z^* greater than 0.77); the base composed of large particles (z^* lower than 0.46); in between the intermediate zone composed of live and dead twigs (mainly twigs in the range of 2 - 6 mm diameter).

The mass proportion of the different size classes of particles, $\Gamma_{k,dry}$, was also estimated:

$$\Gamma_{k,dry} = \frac{m_{k,dry}}{\sum_{k} m_{k,dry}} \quad (17)$$

384 Measurements show a similar distribution of particles for the 3 samples. The shrub were
385 composed of 22.1 ± 0.8 % of leaves, 26.0 ± 2.1 % of twigs ≤ 2 mm in diameter, 18.3 ± 0.9 %
386 of twigs with diameter in the range of 2 - 4 mm, 17.0 ± 1.6 % of twigs with diameter in the
387 range of 4 - 6 mm and 17.0 ± 4.0 % of twigs > 6 mm in diameter. This pre-fire analysis based
388 on size class suggests that about 48.1 % of the fuel elements are prone to burn easily (particle
389 thickness lower than 2 mm), 18 % could burn (2 mm < diameter ≤ 4 mm) and 34 % might not
390 burn (> 4 mm in diameter).

391 Based on these experimental measurements, the distribution of the bulk density within
392 the shrub was established for each particle size class (Table 3). Bulk density refers to the dry
393 mass of fuel elements (leaves and different diameter twigs) per unit volume. These data will be
394 used as input parameters for the numerical study. In the next section the influence of these
395 characteristics on the overall plant flammability is investigated.

396 3.2. Four components of flammability

397 The whole burning process of a shrub of rockrose, from ignition to flameout, is
398 displayed in Fig. 3. The several phases during which the four flammability components were
399 measured through previously defined metrics, are also provided. When being exposed to
400 external radiant heat flux, vegetation temperature increases, desiccation and thermal
401 degradation occur. Combustible gases are released and mixed with ambient air. A small flame,
402 generated by the ignition of this gas mixture by hot glowing particles, quickly engulfed the fuel
403 elements located nearby. Leaves were observed to be the class of particles that first ignites due
404 to their high surface-to-volume ratio. Ignition was always located at the edge of the crown
405 (location where external heat flux is maximum and leaves are the most abundant) but due to the
406 corner configuration of the radiant panels, double ignition could occurred in some rare cases.
407 The fire spread always forward across the crown (leaves and small diameter twigs) and
408 sometimes downward across the intermediate zone (burning greater diameter twigs) depending
409 on the fire heat released. A short (23 ± 10 s) quasi-steady burning period was observed followed
410 by a rapid decay of HRR burnt out. The shrub combustion was incomplete, with char residues
411 and unburnt material located at both the base and intermediate zone of the shrub. Despite the
412 care taken to select plants to be harvested, small discrepancies at particle level (twigs with
413 leaves protruding out of the crown, discontinuity within the crown, trapezoidal instead of
414 spherical crown shape…) yielded to different fire behaviors that will be examined through the
415 flammability components in the following sections.

3.2.1. Ignitability

Ignitability was studied for an external radiant heat flux of 20 $kW.m^{-2}$ as would happen when a flame front, driven by buoyancy effects, approaches vegetation [94]. The difference of importance between the present work and previous studies conducted on full shrubs is that, in the latter, ignition was piloted and performed using a flame at the base of the plant [10, 18, 30-43] instead of auto-ignition. The air drying process at room temperature, resulted in shrub foliar MC in the range of 4-18% on dry basis depending on the initial MC of the samples and drying time. The MC of the particles of other size classes was higher than the one of the leaves. For instance, the corresponding MC for the smaller twigs (diameter < 2 mm) was in the range of 10-45 %. The larger the fuel element diameter, the higher the MC. Even after drying, the shrubs with foliar MC greater than 20% did not burn entirely once ignited and these fire tests were not considered for the flammability study. Even under these low foliar MC conditions, ignitability was difficult to assess using external radiant heat flux only as ignitor. Other works also observed flame extinguishment before much of the plant burned and thus used a pilot flame as ignition source [21] often combined with wind [52, 53] in order to observe sustained combustion of the vegetation samples. The TTI dependence on the MC of the leaves is plotted on Fig. 4 for shrubs harvested in autumn and summer. Despite their scattering (R^2=0.585), the data exhibit an increase of the TTI with increasing MC. The reasons of this scattering can be found in the impossibility to have by nature strictly identical test specimen when working with unmodified plants. The slight changes existing between the structure (position of the leaves within the crown) of the different shrub samples was observed to influence ignitability. The increase of MC decreases the shrub ignitability by requiring more energy for preheating of the fuel and for water evaporation, in accordance with literature [24, 43, 95, 96]. Previous flammability tests [14] conducted on various Mediterranean natural fuels, using ignition apparatus, also found a linear relationship between ignitability and moisture content. Nevertheless, the bulk density of the vegetation samples considered in these small-scale fire tests tends to be overestimated compared to the one of full plants. In another work [23], the authors conducted experimental study submitting live leaves of various species with MC in the range of 35-200% to very high heat fluxes from a flame (80-140 kW/m^2). They concluded that both TTI and ignition temperature showed no dependence on foliar MC. Nevertheless, fire tests carried out at high external radiant heat flux (≥50 kW/m^2) or very high mixed convective-radiative heat flux (pilot flame) [11, 21, 52, 53] may tend to mask the possible differences between samples at different foliar MC levels because too rapid ignition occurs [9, 37]. Ignitability was already observed to

449 be highly dependent on the type of ignition source and scale [11, 96]. Babrauskas [97] also
450 discussed the effects of the variety of external heat sources on ignition of vegetation.
451 Unfortunately, the test procedure and particularly the ignition method for plants parts and
452 furthermore for full scale shrubs is not standardized yet. As a result, a wide range of radiation
453 levels (15-50 kW/m²) can be found in the literature. Furthermore, many studies provide the
454 temperature of the radiant heater instead of heat flux and the comparison is not easy. Martin et
455 al. [5] first suggested that ignitability should be described in terms of time to ignition per rate
456 of energy per unit area in order to take into account the heat flux impinging on the vegetation
457 sample.

458 *3.2.2. Combustibility*

459 Combustibility was defined in terms of both fire growth and peak HRR. A subset of the
460 data, excluding samples of shrub of rockrose harvested in summer, was considered for the study
461 of combustibility, sustainability and consumability due to large difference in crown structure
462 compared to other seasons. Indeed, the persistence of flowers and seeds on the early summer
463 shrubs altered significantly their combustion dynamics and resulting global flammability. Once
464 ignited, burning seeds falling on the ground were observed to make a major contribution to the
465 mass loss but a very limited contribution to the heat release. Furthermore, these incandescent
466 fuel elements are prone to generate secondary ignition points within the crown, influencing the
467 overall combustion of the shrub. On the other hand, up to the ignition of the leaves, the behavior
468 of the shrubs containing seeds was not influenced by their presence. For this reason, the data
469 on the TTI of the summer shrubs were kept when ignitability was studied. In whole plant fire
470 tests, the rates of fire growth and heat released are related to the rate of spread of the fire across
471 the sample and this metrics could also be used to study combustibility [5]. The data analysis
472 distinguished three main types of combustibility according to the growth rate and peak HRR.
473 Curves of HRR versus time corresponding to low (α = 0.10 kW.s^{-2}), medium (α = 0.22 kW.s^{-2})
474 and high combustibility (α = 0.52 kW.s^{-2}) are plotted in Fig. 5. The corresponding fires images,
475 taken 30 s after ignition, are provided in Fig. 6. It should be noticed that the values of the fire
476 growth parameter α obtained for the plant composed of fine particles do not match the standard
477 range (NFPA, 92B [98]) of *t*-squared fires typical of fuels encountered in fire safety for
478 buildings (paper, cardboard, foam…) due to the high porosity and low mass of the shrub crown,
479 resulting in much lower flame duration. In the present study, for α values lower than 0.2 kW.s^{-2}
480 , the fire growth rate was considered as slow (whereas it corresponds to ultrafast fire growth
481 for building materials). The fire spread across the crown was slow and flames were observed to

travel from a branch supporting leaves to another one, resulting in low average peak HRR of 100 ± 5 kW. Consequently, the resulting combustibility was defined as low. Medium fire growth rate and moderate combustibility were observed for α values in the range of 0.2-0.4 $kW.s^{-2}$. The fire spread horizontally from the ignition zone towards the opposite edge of the crown with average peak HRR of 188 ± 27 kW. Finally, for α values higher than 0.4 $kW.s^{-2}$, the fire spread horizontally at a fast rate throughout the entire thin classes of particles located within the crown and then spread vertically downwards through the thicker classes thanks to a higher heat feedback towards the base of the shrub. Combustibility was high and the fire consumed larger diameter particles with high heat release rate (average peak HRR of 257 ± 63 kW). It should be pointed out that the linear relationship between peak HRR and peak MLR exhibits a regression value of the heat of combustion of 13.9 $MJ.kg^{-1}$ ($R^2 = 0.911$).

The fire growth parameter was found to strongly depend on the quantity of foliar biomass above the ignition location. The greater the amount of fuel, the greater the fire growth parameter. When ignition occurs in the region located between the bottom and the middle of the crown, the convective heating of the fuel elements by flame impingement along the full crown height cause a fast fire growth rate that maximize the heat transfer mechanisms. In the following, ignition that occurred in this region will be called as “favorable” whereas ignition located above it will be called as “unfavorable”.

In the present study, the combustibility was assessed using two characteristics of the HRR, namely its growth rate and peak value. Previous studies [8, 9, 11-13, 18, 19, 21, 40, 46, 99] used flame height or maximum air temperature above the sample (which depends on the placement of the thermocouples) that are not relevant descriptors. Indeed, combustibility was defined as how well or rapidly a fuel burns [4]. If HRR cannot be evaluated, the metrics used should be rather based on a rate such as the rate of fire spread across the sample, the rate of temperature increase of the fuel material or better the MLR. Indeed, the MLR can also be used as metrics for combustibility (and not consumability [9, 11, 21]), since it is related to HRR by a constant (effective heat of combustion). As already pointed out [9], the standardization among test procedures to assess the flammability components is necessary.

3.2.3. Sustainability

After growth, the fire reached a short quasi-steady burning stage. The data exhibit that flame duration is related to combustibility and decreases with increasing fire growth parameter and peak HRR (Fig. 7). Data also shows scattering for the reasons previously given for the

ignitability study. Flame duration (FD) in the range of 80 - 120 s were observed for low peak HRR (≤ 150 kW), while shorter FD (around 40 s) were obtained for high peak HRR (≥ 210 kW). Sustainability was also found to depend on the amount of fuel elements present above the ignition location. Indeed, under favorable ignition conditions, the flame quickly engulfed most of the shrub crown resulting in a short FD and high combustibility (high fire growth parameter and peak HRR). Conversely, unfavorable ignitions resulted in slow horizontal propagation. In this case, heat transfers to the unburnt particles are mainly dominated by radiation since the flame did not impinge these fuel elements. The fire could stop because of fuel discontinuity which was too large to result in significant convective heat transfer. Such regime of fire spread exhibited slow rate of spread, long FD and low peak HRR. Authors generally agree on the definition of sustainability that is easy to estimate from direct visual observations or from measurements of various quantities (temperature above threshold). Nevertheless, the wide variety of scales and experimental procedures render the comparison difficult. Indeed, FD is highly dependent on the mass of the fuel, presence of wind but also on ignition characteristics and heat release to sustain combustion of the plant.

3.2.4. Consumability

In order to provide an detailed representation of the particle size classes involved in the combustion process, the fuel consumption at particle level was estimated from the residual mass fraction. It is defined as:

$$\tau_{k,dry}(z^*) = \frac{m^r_{k,dry}(z^*)}{m_{k,dry}(z^*)} \quad (18)$$

where $m^r_{k,dry}$ represents the mass of remaining fuel of the *k*-class of particles on dry basis. Pre-fire (3 samples) and post-fire (test 15) comparison of the distribution along the non-dimensional height (z*) of mass fractions is provided in Fig. 8 for the different classes of particles. Since these characterization measurements consist of destructive sampling, the shrubs to be burnt could unfortunately not be characterized using this method. The use of LIDAR-based technique should be a suitable alternative for the estimation of fuel element distribution within the vegetation [100]. In this particular fire test (Peak HRR of 264 kW), the total fuel consumption ratio was 42%. For most of the fire tests, the crown ($z^* > 0.77$) was fully consumed and the intermediate zone was partially consumed ($0.6 > z^* > 0.77$). Compared to initial mass fractions, the lower values measured in the burnt shrub, indicates that all the foliage and part of the

particles lower than 6 mm in diameter were burnt while the 6 - 25 mm size class did not undergo thermal degradation.

Consumability was also evaluated from the total quantity of fuel consumed by the fire tests. The effect of foliar moisture content on fuel consumption ratio (FCR) is displayed in Fig. 9. The FCR holds a decreasing trend with increasing MC of the leaves in agreement with previous studies [30, 43, 47]. These results suggest that MC alters the thermal degradation processes as a fire retardant. The average mass lost for all experiments was 0.52 ± 0.2 kg which is equivalent to a fuel consumption ratio of 25 ± 8%. Observations during experiments and characterization at the particle level show that the mass was quasi exclusively consumed in the crown which is mainly composed of fine fuel elements (leaves and 0 - 2 mm diameter twigs) that represent 35% of the total dry mass of the shrub. Based on the characterization study and the FCR values obtained, the consumability can be categorized into the three basic types. A FCR below 18% indicates that the leaves were not fully consumed. The fire did not spread across the whole crown resulting in a low consumability. A medium consumability proceeds from a FCR in the range of 18 - 33%, where all the leaves and part of the 0 - 2 mm class particles in the crown were consumed. Finally, FCR greater than 33% indicates a full consumption of the crown and a part of the classes of particles in the range of 0 - 4 mm located within the intermediate zone of the shrub of rockrose. The fuel elements larger than 4 mm were partly consumed only when the peak of HRR was high enough (250 ± 10 kW). It should be noted that fire tests were carried out on conditioned shrub and the initial dry mass could not be measured but only estimated from the wet mass, MC and distribution of each particles size class. Thus, the uncertainty related to the estimation of the dry mass directly affects the calculation of the consumed mass fraction.

3.3. Characterization of different flammability regimes

The same variables as the one used for metrics for the components (FD, peak HRR, peak MLR, fire growth parameter and FCR) were used as input parameters of PCA, except for ignitability where ignition location variable was introduced. Indeed, the use of TTI as a variable for the analysis did not allow to distinguish group tests with similar flammability. When using ignition location instead of TTI, two fire tests from the same cluster exhibited more similar flammability regimes than two tests from different clusters. The concept of flammability is thus revisited in the present approach. A variable of great importance, linked to the random ignition location, is introduced. Indeed, working with natural shrub samples, that show discrepancies,

introduce supplementary difficulties compared to studies carried out at the lower scales, with more similar samples (isolated fuel elements or leafy branch). If strictly identical shrub samples were considered and ignition always occurred in the same area (which is not possible with unmodified vegetation), the TTI would have been an important factor in differentiating the flammability regimes from PCA. In the present study, the ignition location occurred in different areas according to the crown structure and significantly influenced the resulting flammability. When ignition occurs in the region located between the bottom and the middle of the crown, the convective heating of the fuel elements by flame impingement along the full crown height drastically increases the heat transfer mechanisms and causes a fast fire growth rate. PCA reveals that three principal components (PC) explain a total of 87% of the variance (Fig. 10.a). PC 1 explains 54% of the variation in the data. The fire growth parameter, peak HRR, peak MLR characterize PC1 which is therefore representative of both combustibility and sustainability. Ignition location and FCR characterize PC 2 (19% of the variance) and PC3 (14% of the variance, not shown in Fig. 10.a), respectively. Sustainability and combustibility are negatively correlated (opposed). Indeed, the shrub samples exhibiting high combustibility during fire tests typically sustained flame for a shorter duration. The projection of the combustion experiments on the factorial map in the plane (PC 1, PC 2) revealed four clusters of fire tests (Fig. 10.b). Color and black markers refer to single experiment and barycenter of the corresponding flammability group, respectively. Four types of flammability were identified for this plant species:

- The first group (circles) corresponds to fire tests with low flammability, low combustibility (α values lower than 0.2 $kW.s^{-2}$ and a low peak HRR of 83.9 ± 20 kW), high sustainability (very long FD of 100 ± 14 s) and low consumability (weak FCR of 18.9 ± 3.0%). Combustion solely involves leaves and 0-2 mm diameter twigs.
- The second group (squares) is the group of medium flammability with medium combustibility (α values in the range of 0.2 - 0.4 $kW.s^{-2}$, medium peak HRR of 188 ± 27 kW), high sustainability (long FD of 77 ± 10 s) and moderate consumability (FCR of 23 ± 5%). Combustion involves leaves and particles size class up to 4 mm in diameter.
- The third group (diamonds) is characterized by high combustibility (α values greater than 0.4 $kW.s^{-2}$, high peak HRR of 228 ± 15 kW), low sustainability (short FD of 44 ± 9 s) and moderate consumability (moderate FCR (25 ± 6%)). This high flammability with low sustainability group involves the same classes of particles as the medium flammability.

- The last group (triangles) exhibits high combustibility (α values greater than 0.4 $kW.s^{-2}$, very high peak HRR of 384 ± 99 kW), high sustainability (long FD of 70 ± 14 s) and high consumability (high FCR of 32 ± 4%). This high flammability with high sustainability (or hot flammability under the evolutionary concept define by Pausas [17]) includes consumption of particles with diameter greater than 4 mm.

Four regimes of flammability were defined for shrubs of rockrose within the same range of size and shape. Despite a similar shape of the shrub samples, small changes in their structure can significantly affect how they are heated by both convection and radiation and subsequently their flammability as pointed out by [9, 47, 66-70, 101]. The differences between the different flammability regimes are mainly explained by the ignition position, the proportion of the thin fuel elements within the crown and the radiant exposure time. Unfavorable ignition causes low or medium flammability, while favorable ignition results in high flammability. The structure of the vegetation explains the discrepancies between low and medium flammability where estimated foliar bulk density were 2.35 ± 0.64 $kg.m^{-3}$ and 4.65 ± 0.72 $kg.m^{-3}$, respectively. A low bulk density tends to decrease the potential heat release and related fire spread across the shrub crown. In the case of high flammability, the difference between low and high sustainability regimes is mainly caused by radiant exposure time. For the high flammability with high sustainability regime, long exposure time (>400 s) allowed relatively more preheating and desiccation of the plant. The MC of the overall particle size classes was thus considerably reduced when ignition occurs, resulting in high consumability. Indeed, the thermal degradation also occurred for twigs greater than 4 mm in diameter. For shorter exposure time (high flammability with low sustainability), these large diameter twigs did not receive enough heat to achieve desiccation and reach ignition.

3.4. Simulation results

The characterization of the shrub detailed in the previous section (distribution of bulk density of all fuel particle classes and their related MC) provided necessary data for the model inputs. We first used a rectangular grid to model the shrub based on this characterization. However, the cube-based mesh did not match perfectly a shrub's envelope and the crown bulk density was underestimated at the edges. A more suitable model for the geometry, composed of six superposed 0.15 m high frustums with varying radius along the height, were used instead of cubes. Each frustum encompasses 6 fuel layers corresponding to the 6 particle size classes.

The dry bulk density ρ_{bk} of each particle size classes at the mean height of a frustum, z, was determined from the mass measurements (Table 3) by:

$$\rho_{bk}(z) = \frac{m_{k,dry}(z)}{V(z)} \tag{19}$$

where $V(z)$ represents the volume of the frustum and $m_{k,dry}(z)$ is the mass on dry basis of the k-class of particles in the frustum. The grid resolution needed to perform the simulations was estimated from two characteristic length scales associated with two physical phenomena involved in the combustion. The first one corresponds to the extinction length, δ_R, which represents the absorption of radiation by vegetation. δ_R is given by:

$$\delta_R = \frac{4}{\beta_k \sigma_k} \tag{20}$$

The grid size used within the shrub, dx_b must be of the order of one fifth of δ_R [80, 102]. The grid resolution d_x in the gas phase region (flame and buoyant plume) is related to the diameter of the fire, z_c, which represents the second characteristic length scale. McGrattan et al. [58] proposed the following relationship to determine z_c:

$$z_c = \left(\frac{\dot{q}}{\rho_\infty c_p T_\infty \sqrt{g}}\right)^{\frac{2}{5}} \tag{21}$$

where $\dot{q}$, ρ_∞, $c_{p,}$ T_∞ and g are the HRR, the density, specific heat and temperature of the ambient air and the gravitational acceleration, respectively. The authors suggested a ratio z_c/d_x in the range of 4 - 16. The extinction length was calculated from the numerical shrub characteristics. A value of 0.144 m was obtained for δ_R which leads to a grid size lower than 0.029 m. Concerning the mesh size for the flow, z_c was calculated from the peaks of HRR obtained for the four flammability regimes. The minimum value of $z_c = 0.356$ m was obtained for the low flammability fire tests with a measured average peak HRR of 100 kW. The value of z_c suggested d_x in the range of 0.022-0.089 m. Based on these results, the mesh size was chosen as the minimum of d_x and dx_b (0.02 m) in both domains for the shrub and surrounding gas. The whole computational domain includes the extraction hood and the radiant panels in order to fully match the experimental conditions. A preliminary simulation was carried out in order to check the agreement between predicted and measured radiant heat flux density from the radiant panels heated at 520°C. WFDS succeeded to predict auto ignition of the shrub, but the simulated flame did not release enough heat to sustain the combustion and fire spread across

668 the shrub. Thereby, a piloted ignition was added, consisting of fuel elements kept at a
669 temperature of 1000°C for a given time. The ignitor was set on when the predicted pyrolysis
670 mass loss due to preheating had reached the experimental one. Its duration (15 s) was then fitted
671 for the fire to sustain spread. As a first step to investigate the numerical burning of a shrub, the
672 simulations performed with WFDS were conducted for the high flammability with low
673 sustainability regime which experimental results exhibited the best reproducibility. The ignitor
674 was set in the lower part of the crown and its volume (10×20×20 cm^3) corresponds to the size
675 of the flame observed during the experiments at ignition. This location corresponds to a
676 favourable ignition as mentioned in the experimental section.

677 Based on the experiments, average moisture contents were used for the different size classes
678 of particles (Table 3). The comparison of the predicted and measured fire spread at different
679 times is provided in Fig. 11. A 200 $kW.m^{-3}$ iso-contour of volumetric heat release rate was
680 retained for the visual representation of the flame that nearly corresponds to a 500°C iso-
681 surface. The corresponding predicted and measured HRR and MLR over time are plotted in
682 Fig. 12. The predicted HRR is the sum of the heat released by gas phase reactions within the
683 flame and solid phase due to the char oxidation. The main discrepancy in the curves compared
684 to measurements can be found in the presence of a plateau just after ignition. The reasons for
685 this difference can be attributed to the Arrhenius law used for the formulation of the thermal
686 degradation. The predicted peak HRR (215 kW) compares favourably to the measured one (226
687 ± 24 kW). The predicted (and measured) mass consumed and peak MLR were 0.36 kg (0.58 ±
688 0.17 kg) and 0.012 $kg.s^{-1}$ (and 0.015 ± 0.003 $kg.s^{-1}$), respectively. The prediction of the flame
689 duration (42 s) is also in agreement with the one measured during the experiments (44 ± 9 s).
690 The faster predicted decay phase may be caused by an overestimation of the particles cooling
691 with fresh air after the flameout. The resulting mass consumption is underestimated due to a
692 rapid extinction of the char after the flameout. As far as FCR is concerned, the predicted value
693 (31%) is close to measurements (32 ± 8%). Despite differences during fire growth and decay
694 phases, the model predictions are in good agreement with experimental data. The vertical
695 distribution of the bulk density of the thin fuel elements of the shrub of rockrose ($\rho_b <$
696 $6\ kg/m^3$) is comparable to the one of another shrub species (chamise) considered in previous
697 studies [30, 78] combining fire experiments and numerical simulation based on large eddy
698 simulation. The thermal degradation of the fuel elements predicted in the present approach is
699 consistent with these previous works. For a shrub of chamise, predicted (and measured) mass
700 consumed and peak MLR were 0.49 kg (0.48 ± 0.11 kg) and 0.044 $kg.s^{-1}$ (0.030 ± 0.01 $kg.s^{-1}$),

701 respectively. Due to the different ignition procedure (pilot flame at the base of the shrub) the
702 resulting MLR and total mass consumed were greater for the chamise fire tests. Terrei et al.
703 [21] also found a good agreement between WFDS predictions and measurements of both mass
704 losses and temperatures at the scale of a branch. The present results confirm that WFDS can
705 provide an accurate assessment flammability for a full scale plant.

706

707 ## 4. Conclusion

708 In the present study, experimental data was collected on the structure and flammability of
709 individual shrubs of rockrose. The use of oxygen consumption calorimetry on full-scale plants
710 was a substantial step forward to quantify flammability and improve the knowledge on the
711 combustion of these natural fuels.

712 Shrubs of rockrose were characterized to obtain accurate measures of the proportion and
713 distribution of mass for different size classes of particles from base to crown. The latter
714 embodies thin fuel elements that were observed to play a critical role during combustion and
715 represent the main part of the consumed biomass. The flammability of the shrubs was analyzed
716 using some of the usual measurements. The time to ignition, used as metric for ignitability,
717 decreases with the foliar MC. The HRR (growth rate and Peak value) and the flame duration,
718 indicators combustibility and sustainability, respectively, were influenced by the location of the
719 ignition within the crown. The lower the position, the higher the peak HRR and the shorter the
720 flame duration. The FCR, metrics for consumability, increases with decreasing foliar MC. The
721 comparison to previous experimental studies highlighted the necessity of standardization
722 among test procedures to assess the flammability components of plants, more particularly at
723 full scale. Finally, a statistical analysis exhibited four types of flammability depending on the
724 ignition zone, HRR and consumed mass of thin fuel elements.

725 The shrub characterization and fire experiments carried out were used as a comparison basis
726 for the predictions of WFDS. This study highlighted the capacity of WFDS to predict the main
727 fire characteristics (peak HRR, flame duration and consumption rate). However, simulations
728 results showed a plateau in the HRR after the ignition that alters the predicted fire growth. The
729 extinction of the char smoldering phase was too fast, probably due to an overestimation of the
730 convective cooling. An investigation on the causes of these discrepancies through more
731 thorough investigation of the degradation laws needs to be addressed.

Experimental results will need to be scaled-up to field conditions and include the interaction of multiple shrubs. The large scale heat release apparatus also offers the possibility to expand the study beyond a single plant and explore the interactions among several shrubs on the fire behavior and flammability. Future works need also to take into account litter fuels at the base of the shrub that were observed to contribute significantly to shrub flammability [49].

Acknowledgements: The authors are grateful to David Perez-Merino of the Université de Nancy, for his valuable contribution on the WFDS simulation runs.

References

[1] W.M. Jolly, M.A. Cochrane, P.H. Freeborn, Z.A. Holden, T.J. Brown, G.J. Williamson, D.M. Bowman, Climate-induced variations in global wildfire danger from 1979 to 2013, Nature Communications 6 (2015) 7537.
[2] J. San-Miguel-Ayanz, T. Durrant, R. Boca, G. Libertà, A. Branco, D.d. Rigo, D. Ferrari, P. Maianti, T.A. Vivancos, H. Costa, F. Lana, P. Löffler5, D. Nuijten, T. Leray, Forest fires in Europe, Middle East and North Africa 2017, Publications Office of the European Union, Luxembourg, 2018.
[3] NICC, Wildland Fire Summary and Statistics Annual Report 2017, National Interagency Coordination Center, Boise, Idaho, 2017.
[4] H.E. Anderson, Forest fuel ignitibility, Fire Technology 6 (1970) 312-319.
[5] R. Martin, D. Gordon, M. Gutierrez, D. Lee, D. Molina, R. Schroeder, D. Sapsis, S. Stephens, M. Chambers, Assessing the flammability of domestic and wildland vegetation, in: M. Society of American Foresters: Bethesda (Ed.) Proceedings of the 12th conference on fire and forest meteorology, Jekyll Island, GA, 1994, pp. 130–137.
[6] E.H. Mak, Measuring foliar flammability with the limited oxygen method, Forest Science 17 (1988) 253–259.
[7] M. Guijarro, C. Hernando, C. Díez, E. Martínez, J. Madrigal, C. Lampin-Cabaret, L. Blanc, P.Y. Colin, P. Pérez-Gorostiaga, J.A. Vega, Flammability of some fuel beds common in the South-European ecosystems, IV International Conference on Forest Fire Research, Coimbra, Portugal, 2002.
[8] A. Ganteaume, J. Marielle, L.-M. Corinne, C. Thomas, B. Laurent, Effects of vegetation type and fire regime on flammability of undisturbed litter in Southeastern France, Forest Ecology and Management 261 (2011) 2223-2231.
[9] R.H. White, W.C. Zipperer, Testing and classification of individual plants for fire behaviour: plant selection for the wildlandurban interface, International Journal of Wildland Fire 19 (2010) 213-227.
[10] M.P. Plucinski, W.R. Catchpole, Predicting ignition thresholds in litter layers, MODSIM 2001: International Congress on Modelling and Simulation, Canberra, Australia, 2001, pp. 967–971.
[11] J. Madrigal, E. Marino, M. Guijarro, C. Hernando, C. Díez, Evaluation of the flammability of gorse (Ulex europaeus L.) managed by prescribed burning, Annals of Forest Science 69 (2012) 387-397.

[12] V.M. Santana, R.H. Marrs, Flammability properties of British heathland and moorland vegetation: models for predicting fire ignition, Journal of environmental management 139 (2014) 88-96.
[13] A.L. Behm, M.L. Duryea, A.J. Long, W.C. Zipperer, Flammability of native understory species in pine flatwood and hardwood hammock ecosystems and implications for the wildlandurban interface, International Journal of Wildland Fire 13 (2004) 355-365.
[14] A.P. Dimitrakopoulos, K.K. Papaioannou, Flammability Assessment of Mediterranean Forest Fuels, Fire Technology 37 (2001) 143-152.
[15] A. Ganteaume, M. Jappiot, C. Lampin, M. Guijarro, C. Hernando, Flammability of some ornamental species in wildland-urban interfaces in southeastern France: laboratory assessment at particle level, Environmental management 52 (2013) 467-480.
[16] D.W. Schwilk, Dimensions of plant flammability, New Phytologist 206 (2015) 486-488.
[17] J.G. Pausas, J.E. Keeley, D.W. Schwilk, Flammability as an ecological and evolutionary driver, Journal of Ecology 105 (2017) 289-297.
[18] L.D. Prior, B.P. Murphy, D.M. Bowman, Conceptualizing Ecological Flammability: An Experimental Test of Three Frameworks Using Various Types and Loads of Surface Fuels, Fire 1 (2018) 18.
[19] S.H. Essaghi, M.; Yessef, M.; Dehhaoui, M.; El Amarty, F., Assessment of Flammability of Moroccan Forest Fuels: New Approach to Estimate the Flammability Index, Forests 8 (2017).
[20] P. Jaureguiberry, G. Bertone, S. Díaz, Device for the standard measurement of shoot flammability in the field, Austral Ecology 36 (2011) 821-829.
[21] L. Terrei, A. Lamorlette, A. Ganteaume, Modelling the fire propagation from the fuel bed to the lower canopy of ornamental species used in wildland–urban interfaces, International Journal of Wildland Fire 28 (2019) 113-126.
[22] D.R. Weise, R.H. White, F.C. Beall, M. Etlinger, Use of the cone calorimeter to detect seasonal differences in selected combustion characteristics of ornamental vegetation, International Journal of Wildland Fire 14 (2005) 321-338.
[23] T.H. Fletcher, B.M. Pickett, S.G. Smith, G.S. Spittle, M.M. Woodhouse, E. Haake, D.R. Weise, Effects of moisture on ignition behavior of moist California chaparral and Utah leaves, Combustion Science and Technology 179 (2007) 1183-1203.
[24] G.M. Davies, C.J. Legg, Fuel Moisture Thresholds in the Flammability of Calluna vulgaris, Fire Technology 47 (2011) 421-436.
[25] S. McAllister, D.R. Weise, Effects of Season on Ignition of Live Wildland Fuels Using the Forced Ignition and Flame Spread Test Apparatus, Combustion Science and Technology 189 (2017) 231-247.
[26] K.J. Simpson, B.S. Ripley, P.-A. Christin, C.M. Belcher, C.E.R. Lehmann, G.H. Thomas, C.P. Osborne, Determinants of flammability in savanna grass species, Journal of Ecology 104 (2016) 138-148.
[27] D.M.J.S. Bowman, B.J. French, L.D. Prior, Have plants evolved to self-immolate?, Frontiers in Plant Science 5 (2014).
[28] B.M. Pickett, C. Isackson, R. Wunder, T.H. Fletcher, B.W. Butler, D.R. Weise, Experimental measurements during combustion of moist individual foliage samples, International Journal of Wildland Fire 19 (2010) 153-162.
[29] V. Babrauskas, Effective heat of combustion for flaming combustion of conifers, Canadian Journal of Forest Research 36 (2006) 659-663.
[30] A. Dahale, S. Ferguson, B. Shotorban, S. Mahalingam, Effects of distribution of bulk density and moisture content on shrub fires, International Journal of Wildland Fire 22 (2013) 625-641.

[31] M.G. Etlinger, F.C. Beall, Development of a laboratory protocol for fire performance of landscape plants, International Journal of Wildland Fire 13 (2004) 479-488.
[32] G. Pellizzaro, P. Duce, A. Ventura, P. Zara, Seasonal variations of live moisture content and ignitability in shrubs of the Mediterranean Basin, International Journal of Wildland Fire 16 (2007) 633-641.
[33] F.X. Jervis, G. Rein, Experimental study on the burning behaviour of Pinus halepensis needles using small-scale fire calorimetry of live, aged and dead samples, Fire and Materials 40 (2016) 385-395.
[34] N. Bal, Forty years of material flammability: An appraisal of its role, its experimental determination and its modelling, Fire Safety Journal 96 (2018) 46-58.
[35] P.M. Fernandes, M.G. Cruz, Plant flammability experiments offer limited insight into vegetation–fire dynamics interactions, New Phytologist 194 (2012) 606-609.
[36] T. Barboni, L. Leonelli, P.-A. Santoni, V. Tihay-Felicelli, Influence of particle size on the heat release rate and smoke opacity during the burning of dead Cistus leaves and twigs, Journal of Fire Sciences 35 (2017) 259-283.
[37] J. Madrigal, C. Hernando, M. Guijarro, A new bench-scale methodology for evaluating the flammability of live forest fuels, Journal of Fire Sciences 31 (2013) 131-142.
[38] V. Tihay-Felicelli, P.-A. Santoni, T. Barboni, L. Leonelli, Autoignition of Dead Shrub Twigs: Influence of Diameter on Ignition, Fire Technology 52 (2016) 897-929.
[39] A.C. Dibble, R.H. White, P.K. Lebow, Combustion characteristics of north-eastern USA vegetation tested in the cone calorimeter: invasive versus non-invasive plants, International Journal of Wildland Fire 16 (2007) 426-443.
[40] S.V. Wyse, G.L.W. Perry, D.M. O'Connell, P.S. Holland, M.J. Wright, C.L. Hosted, S.L. Whitelock, I.J. Geary, K.J.L. Maurin, T.J. Curran, A quantitative assessment of shoot flammability for 60 tree and shrub species supports rankings based on expert opinion, International Journal of Wildland Fire 25 (2016) 466-477.
[41] G.H. Damant, S. Nurbakhsh, Christmas trees—what happens when they ignite?, Fire and Materials 18 (1994) 9-16.
[42] D. Stroup, L. DeLauter, J. Lee, G. Roadarmel, Scotch pine Christmas tree fire tests, Report of Test FR 4010. USDC, National Institute of Standards and Technology, Gaithersburg, MD, 1 December 1999, 1999.
[43] V. Babrauskas, Chastagner G, S. E, Flammability of cut Christmas trees, IAAI Annual general meeting, Atlantic City, NJ, 2001, pp. 1–29.
[44] V. Babrauskas, Heat release rates, The SFPE handbook of fire protection and engineering, National Fire Protection Association, Quincy, MA, 2002, pp. 1–37.
[45] D.D. Evans, R.G. Rehm, E.S. Baker, Physics-Based Modeling for WUI Fire Spread: Simplified Model Algorithm for Ignition of Structures by Burning Vegetation, NIST Interagency/Internal Report (NISTIR) - 7179, NIST, Gaithersburg, MD, 2004.
[46] A. Long, B. Hinton, W. Zipperer, A. Hermansen-Baez, A. Maranghides, W. Mell, Quantifying and ranking the flammability of ornamental shrubs in the southern United States, Fire Ecology and Management Congress, The Association for Fire Ecology and Washington State University Extension, San Diego, CA, 2006, pp. 1-3.
[47] K. Zhou, J. Jia, J. Zhu, Experimental research on the burning behavior of dragon juniper tree, Fire and Materials 42 (2018) 173-182.
[48] E. Baker, J. Woycheese, Burning characteristics of Douglas-fir trees: scaling of individual tree fire based on tree size, Conference papers fire and materials, 2007, 10th international conference, Interscience Communications: London, San Francisco, CA, 2007.
[49] J. Li, S. Mahalingam, D.R. Weise, Experimental investigation of fire propagation in single live shrubs, International Journal of Wildland Fire 26 (2017) 58-70.

[50] R.H. White, D. DeMars, M. Bishop, Flammability of Christmas trees and other vegetation, in: C.J. Hilado (Ed.) Proceedings of the 24th international conference on fire safety, Columbus, OH, 1997, pp. 99-110.
[51] S.L. Stephens, D.A. Gordon, R.E. Martin, Combustibility of selected domestic vegetation subjected to desiccation, Proceedings of the 12th Conference on Fire and Fire Meteorology, Society of American Foresters: Bethesda, MD, Jekyll Island, GA, 1994, pp. 565–571.
[52] W. Tachajapong, J. Lozano, S. Mahalingam, D.R. Weise, Experimental modelling of crown fire initiation in open and closed shrubland systems, International Journal of Wildland Fire 23 (2014) 451-462.
[53] D. Prince, C. Shen, T. Fletcher, Semi-empirical Model for Fire Spread in Shrubs with Spatially-Defined Fuel Elements and Flames, Fire Technology 53 (2017) 1439-1469.
[54] C. Schemel, A. Simeoni, H. Biteau, J. Rivera, J. Torero, A calorimetric study of wildland fuels, Experimental Thermal and Fluid Science 32 (2008) 1381–1389.
[55] J. Madrigal, C. Hernando, M. Guijarro, C. Díez, E. Marino, A.J. De Castro, Evaluation of Forest Fuel Flammability and Combustion Properties with an Adapted Mass Loss Calorimeter Device, Journal of Fire Sciences 27 (2009) 323-342.
[56] P. Bartoli, A. Simeoni, H. Biteau, J.L. Torero, P.A. Santoni, Determination of the main parameters influencing forest fuel combustion dynamics, Fire Safety Journal 46 (2011) 27-33.
[57] A. Simeoni, J.C. Thomas, P. Bartoli, P. Borowieck, P. Reszka, F. Colella, P.A. Santoni, J.L. Torero, Flammability studies for wildland and wildland–urban interface fires applied to pine needles and solid polymers, Fire Safety Journal 54 (2012) 203-217.
[58] K. McGrattan, S. Hostikka, R. McDermott, J. Floyd, C. Weinschenk, K. Overholt, Fire Dynamics Simulator User's Guide. Technical Report NIST Special Publication, 1019-6, National Institute of Standards and Technology, Gaithersburg, Maryland, 2013.
[59] N. Chiaramonti, E. Romagnoli, P.A. Santoni, T. Barboni, Comparison of the Combustion of Pine Species with Two Sizes of Calorimeter: 10 g vs. 100 g, Fire Technology 53 (2017) 741-770.
[60] S. Fehrmann, W. Jahn, J. de Dios Rivera, Permeability Comparison of Natural and Artificial Pinus Radiata Forest Litters, Fire Technology 53 (2017) 1291-1308.
[61] A. Ganteaume, M. Jappiot, T. Curt, C. Lampin, L. Borgniet, Flammability of litter sampled according to two different methods: comparison of results in laboratory experiments, International Journal of Wildland Fire 23 (2014) 1061-1075.
[62] S. Figueroa, J.d.D. Rivera, W. Jahn, Influence of Permeability on the Rate of Fire Spread over Natural and Artificial Pinus radiata Forest Litter, Fire Technology, doi:10.1007/s10694-019-00824-w(2019).
[63] S. Pyne, P. Andrews, R. Laven, Introduction to Wildland Fire, 2nd edition revised ed., John Wiley & sons, inc., New York, 1996.
[64] D.W. Schwilk, Flammability Is a Niche Construction Trait: Canopy Architecture Affects Fire Intensity, the american naturalist 162 (2003) 725-733.
[65] A. Ganteaume, Does plant flammability differ between leaf and litter bed scale? Role of fuel characteristics and consequences for flammability assessment, International Journal of Wildland Fire 27 (2018) 342-352.
[66] M.G. Just, M.G. Hohmann, W.A. Hoffmann, Where fire stops: vegetation structure and microclimate influence fire spread along an ecotonal gradient, Plant Ecology 217 (2016) 631-644.
[67] H.E. Anderson, Relationship of fuel size and spacing to combustion characteristics of laboratory fuel cribs, Research Paper INT-424, USDA Forest Service, Intermountain Research Station, 1990.
[68] M.J. Gollner, Y. Xie, M. Lee, Y. Nakamura, A.S. Rangwala, Burning behavior of vertical matchstick arrays, Comb. Sci. Tech. 184 (2012) 585–607.

[69] M.F. Wolff, G.F. Carrier, F.E. Fendell, Wind-Aided Firespread Across Arrays of Discrete Fuel Elements. II. Experiment, Combustion Science and Technology 77 (1991) 261-289.
[70] W.R. Anderson, E.A. Catchpole, B.W. Butler, Convective heat transfer in fire spread through fine fuel beds, International Journal of Wildland Fire 19 (2010) 284-298.
[71] G.B. Peet, A fire danger rating and controlled burning guide for the Northern Jarrah (Euc Marginata sm) forest of Western Australia, Forests Dept, Perth, (1965).
[72] M.A. Finney, J.D. Cohen, J.M. Forthofer, S.S. McAllister, M.J.J. Gollner, D.J. Gorham, K. Saito, N.K. Akafuah, B.A. Adam, J.D. English, Role of buoyant flame dynamics in wildfire spread, Proceedings of the National Academy of Sciences 112 (2015) 9833-9838.
[73] N.D. Burrows, Flame residence times and rates of weight loss of eucalypt forest fuel particles, International Journal of Wildland Fire 10 (2001) 137-143.
[74] V. Babrauskas, R.D. Peacock, Heat release rate: the single most important variable in fire hazard, Fire Saf. J. 18 (1992) 255–272.
[75] J. Madrigal, M. Guijarro, C. Hernando, C. Díez, E. Marino, Estimation of Peak Heat Release Rate of a Forest Fuel Bed in Outdoor Laboratory Conditions, Journal of Fire Sciences 29 (2011) 53-70.
[76] B. Porterie, J.L. Consalvi, A. Kaiss, J.C. Loraud, Predicting Wildland Fire Behavior and Emissions Using a Fine-Scale Physical Model, Numerical Heat Transfer, Part A: Applications 47 (2005) 571-591.
[77] D. Morvan, J.L. Dupuy, F. Pimont, R.R. Linn, Numerical study of grassland fires behaviour using a physical multiphase formulation, Forest Ecology and Management 234 (2006) S90-S90.
[78] S. Padhi, B. Shotorban, S. Mahalingam, Computational investigation of flame characteristics of a non-propagating shrub fire, Fire Safety Journal 81 (2016) 64-73.
[79] Y. Perez-Ramirez, W.E. Mell, P.A. Santoni, J.B. Tramoni, F. Bosseur, Examination of WFDS in Modeling Spreading Fires in a Furniture Calorimeter, Fire Technology 53 (2017) 1795–1832.
[80] W. Mell, A. Maranghides, R. McDermott, S.L. Manzello, Numerical simulation and experiments of burning douglas fir trees, Combustion and Flame 156 (2009) 2023-2041.
[81] J.L. Dupuy, J. Maréchal, D. Morvan, Fires from a cylindrical forest fuel burner: combustion dynamics and flame properties, Combustion and Flame 135 (2003) 65-76.
[82] F. Pimont, J.L. Dupuy, R.R. Linn, Coupled slope and wind effects on fire spread with influences of fire size: a numerical study using FIRETEC, International Journal of Wildland Fire 21 (2012) 828-842.
[83] W. Mell, M.A. Jenkins, J. Gould, P. Cheney, A physics-based approach to modelling grassland fires, International Journal of Wildland Fire 16 (2007) 1-22.
[84] J. Dold, A. Simeoni, A. Zinoviev, R. Weber, The Palasca fire, September 2000: Eruption or Flashover?, in: D. Viegas (Ed.), Forest Fire Accidents in Europe, JRC, Ispra, 2009.
[85] S. Lahaye, J. Sharples, C. Hély, T. Curt, Toward safer firefighting strategies and tactics, Toward safer firefighting strategies and tactics, Imprensa da Universidade de Coimbra, Coimbra, 2018.
[86] C. Papió, L. Trabaud, Structural characteristics of fuel components of five Meditarranean shrubs, Forest Ecology and Management 35 (1990) 249-259.
[87] M. Cohen, E. Rigolot, M. Etienne, Modeling fuel distribution with cellular-automata for fuel-break assessment., in: D.X. Viegas (Ed.) IV international conference on forest fire research, Millpress, Rotterdam, Luso, Portugal, 2002.
[88] V. Krivtsov, O. Vigy, C. Legg, T. Curt, E. Rigolot, I. Lecomte, M. Jappiot, C. Lampin-Maillet, P. Fernandes, G.B. Pezzatti, Fuel modelling in terrestrial ecosystems: An overview in the context of the development of an object-orientated database for wild fire analysis, Ecological Modelling 220 (2009) 2915-2926.

[89] G. Heskestad, Similarity Relations for the Initial Convective Flow Generated by Fire, FM Report 72-WA/HT-17, Factory Mutual Research Corporation, Norwood, MA, 1972.
[90] K. Dungan, Performance-Based Approach to Designing and Analyzing Fire Detection Systems, NFPA 72® National Fire Alarm Code®, 2003.
[91] W.J. Parker, Calculations of the Heat Release Rate by Oxygen Consumption for Various Applications, Journal of Fire Sciences 2 (1984) 380–395.
[92] M.L. Janssens, Measuring Rate of Heat Release by Oxygen Consumption, Fire Technol. 27 (1991) 234-249.
[93] F. Morandini, Y. Perez-Ramirez, V. Tihay, P.-A. Santoni, T. Barboni, Radiant, convective and heat release characterization of vegetation fire, International Journal of Thermal Sciences 70 (2013) 83-91.
[94] F. Morandini, X. Silvani, Experimental investigation of the physical mechanisms governing the spread of wildfires, International Journal of Wildland Fire 19 (2010) 570-582.
[95] M.E. Alexander, M.G. Cruz, Assessing the effect of foliar moisture on the spread rate of crown fires, International Journal of Wildland Fire 22 (2013) 415-427.
[96] S. Fares, S. Bajocco, L. Salvati, N. Camarretta, J.-L. Dupuy, G. Xanthopoulos, M. Guijarro, J. Madrigal, C. Hernando, P. Corona, Characterizing potential wildland fire fuel in live vegetation in the Mediterranean region, Annals of Forest Science 74 (2017) 1.
[97] V. Babrauskas, Ignition handbook : principles and applications to fire safety engineering, fire investigation, risk management and forensic science, Fire Science Publishers, Issaquah, WA, 2003.
[98] NFPA92B, Guide for Smoke Management Systems in Malls, Atria, and Large Areas, National Fire Protection Associationn, Quincy, Massachusetts, 2000.
[99] A.M. Gill, P. Zylstra, Flammability of Australian forests, Australian Forestry 68 (2005) 87-93.
[100] F. Pimont, J.-L. Dupuy, E. Rigolot, V. Prat, A. Piboule, Estimating Leaf Bulk Density Distribution in a Tree Canopy Using Terrestrial LiDAR and a Straightforward Calibration Procedure, Remote Sensing 7 (2015) 7995-8018.
[101] P.M. Fernandes, W.R. Catchpole, F.C. Rego, Shrubland fire behaviour modelling with microplot data, Canadian Journal of Forest Research 30 (2000) 889-899.
[102] D. Morvan, J.L. Dupuy, Modeling of fire spread through a forest fuel bed using a multiphase formulation, Combustion and Flame 127 (2001) 1981-1994.

Table 1: Measurements of burning characteristics of whole plants in relation to some flammability components (TTI: Time to ignition; FD: Flame duration; HRR: Heat Release Rate; MLR: Mass Loss Rate; THR: Total Heat Released)

Vegetation species	Ignitability / ignition source	Sustainability	Combustibility	Consumability
[51] Tam junipers	- / 15 s natural gas wand	-	Peak HRR (kW)	-
[11] Gorse shrubs	TTI (s) / flame from pine wood	FD (s)	Rate of temperature increase ($°C.s^{-1}$), HRR ($kW.m^{-2}$), MLR ($kg.s^{-1}$)	Residual mass fraction (%)
[51] Christmas trees	- / paper match	FD (s)	Peak HRR (kW)	Mass consumed (kg, %)
[42] Scotch Pine Christmas trees	- / electric match	-	Peak HRR (kW)	Mass consumed (kg)
[43, 44] Christmas trees	- / small flame to a branch	-	HRR (kW)	-
[31] 6 species of landscape vegetation	- / propane burner	FD (s)	Peak HRR (kW)	Mass consumed (kg)
[50] Christmas trees and ornemental plants	TTI (s) / 8 s match, 20-30s lighter flame, 8 s electric arc, overheated wire	-	Peak HRR (kW)	-
[22] Small shrubs	- / propane burner		Peak HRR (kW)	Mass consumed (kg)
[45, 48] Douglas-fir trees	- / 5-15 s propane torch	FD (s)	Peak HRR (kW)	Mass consumed (kg)
[46] 34 species of ornemental shrubs	TTI (s) / 40 kW burner	FD (s)	Peak HRR (kW)	Mass loss (kg), canopy volume consumed (m^3)
[47] Dragon juniper trees	- / heptane ring fire	FD (s)	MLR ($kg.s^{-1}$)	Mass consumed (%)
[49] Live shrubs	- / surface fire spreading	-	ROS ($m.s^{-1}$), MLR ($kg.s^{-1}$)	Mass consumed (%)
[53] Branches of manzanita shrubs	- / flame from dry excelsior	FD (s)	-	Mass consumed (%)
[Present study] Shrubs of rockrose	TTI (s) / 20 kW/m² radiant panel	FD (s)	HRR (peak kW, growth rate $kW.s^{-2}$), MLR ($g.s^{-1}$)	Mass consumed (%), fuel consumption per particle class (%)

Table 2: Ambiant conditions, plant sample characteristics and fire test properties

Fire Test n°	Air Temp. (°C)	Air RH (%)	Shrub mass (kg)	Crown base height (m)	Total height (m)	Crown diameter (m)	Leaves MC (%)	0-2 MC (%)	Total Mass loss (kg)	THR (kJ)
1	22.9	27.3	2.16	1.04	1.40	0.60	6	10	0.46	6426
2	23.5	26.0	1.50	0.90	1.35	0.60	6	10	0.49	4944
3	27.0	23.8	1.03	0.80	1.10	0.75	6	11	0.15	2368
4	26.0	41.0	1.68	0.95	1.20	0.60	14	31	0.37	4677
5	27.8	37.0	1.97	0.97	1.26	0.85	16	32	0.53	6293
6	25.5	43.4	2.02	0.93	1.31	0.62	15	30	0.38	4517
7	23.0	28.0	1.86	0.99	1.35	0.70	9	40	0.50	5527
8	22.0	31.0	2.30	1.02	1.25	0.74	9	41	0.81	11382
9	22.5	33.3	1.97	0.80	1.40	0.96	9	40	0.43	5730
10	20.9	45.0	2.99	1.00	1.25	0.64	18	44	0.47	6331
11	23.4	39.1	2.50	0.87	1.31	0.65	12	32	0.56	7115
12	23.9	38.7	2.39	0.89	1.25	0.58	12	32	0.81	11302
13	23.0	41.0	1.96	0.95	1.35	0.72	4	16	0.66	8190
14	23.0	43.0	2.39	0.90	1.20	0.75	8	25	0.49	6790
15	23.5	39.5	1.93	1.00	1.30	0.72	8	25	0.74	10579
16	24.8	38.2	0.93	0.85	1.15	0.60	8	25	0.39	6041
17	31.8	37.2	1.75	1.11	1.30	0.79	7	12	0.29	3317
18	31.2	38.2	2.12	0.90	1.32	0.70	5	10	0.31	3000
19	31.2	38.1	0.89	0.83	1.11	0.55	5	10	0.16	1802
20	26.0	45.0	2.23	1.10	1.30	0.65	17	30	0.49	5677
21	31.0	36.0	2.55	1.10	1.35	0.70	18	21	0.28	4605
22	28.0	39.5	2.30	1.15	1.35	0.60	9	18	0.60	7630
23	27.3	43.0	1.97	1.05	1.30	0.55	11	20	0.39	4486
24	27.3	42.8	1.86	1.00	1.20	0.70	13	24	0.59	6706
25	27.3	42.5	2.04	1.00	1.30	0.65	9	14	0.64	8632
26	30.5	36.5	1.83	1.00	1.30	0.69	12	16	0.50	6090
27	29.7	38.7	1.88	0.90	1.20	0.65	6	12	0.71	8730
28	30.0	38.0	2.17	1.05	1.30	0.76	6	7	0.36	4536

Table 3: Average fuel element properties for each class of particle used in WFDS (MC: moiture content; σ: surface area-to-volume ratio, ρ: density; ρ_b: bulk density)

	Leaves	**0-2 mm dead twigs**	**0-2 mm live twigs**	**2-4 mm live twigs**	**4-6 mm live twigs**	**6-25 mm live twigs**
MC (%)	7	2	23	27	35	45
σ (m^{-1})	2081	1733	1733	1000	666	400
ρ ($kg.m^{-3}$)	478	961	961	961	961	961
$\rho_b(0.88 < z^* \leq 1.00)$ ($kg.m^{-3}$)	3.99	0	1.63	0.04	0	0
$\rho_b(0.77 < z^* \leq 0.88)$ ($kg.m^{-3}$)	2.73	0.13	2.45	0.99	0.08	0
$\rho_b(0.65 < z^* \leq 0.77)$ ($kg.m^{-3}$)	1.32	0.31	2.79	2.34	1.07	0
$\rho_b(0.46 < z^* \leq 0.65)$ ($kg.m^{-3}$)	0.52	1.04	1.09	2.46	2.95	0.37
$\rho_b(0.34 < z^* \leq 0.46)$ ($kg.m^{-3}$)	0.48	1.04	0.49	2.13	3.83	3.54
$\rho_b(0.23 < z^* \leq 0.34)$ ($kg.m^{-3}$)	0.30	0.38	1.18	1.41	2.48	12.27
$\rho_b(0.00 < z^* \leq 0.23)$ ($kg.m^{-3}$)	0	0	0	N/A	N/A	N/A

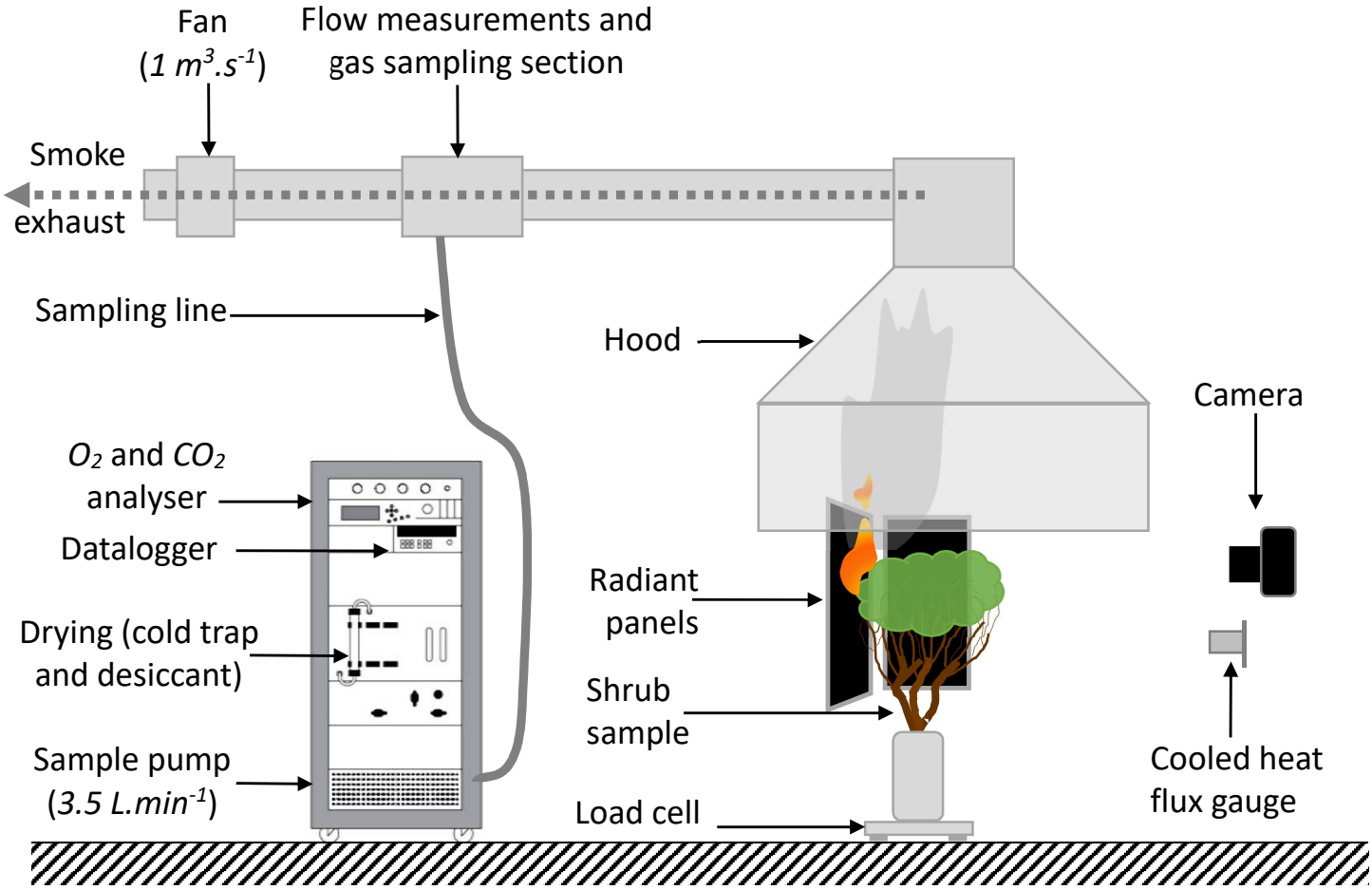

Fig. 1. Layout of the experimental setup

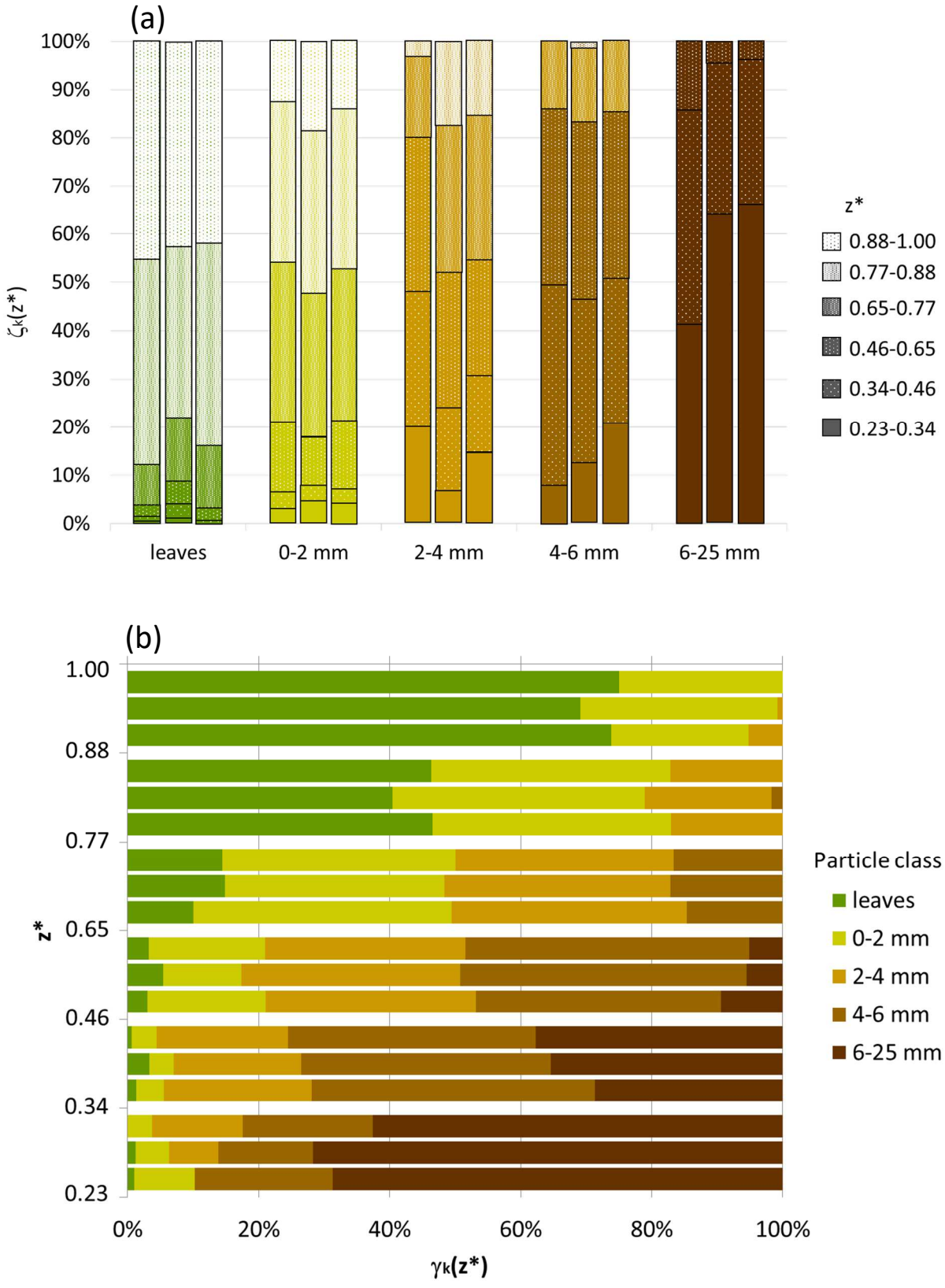

Fig. 2. Characterization of 3 shrubs of rockrose (a) mass distribution of the different particle size classes as function of non-dimensional height z^* and (b) mass fraction versus height for the different particle size classes

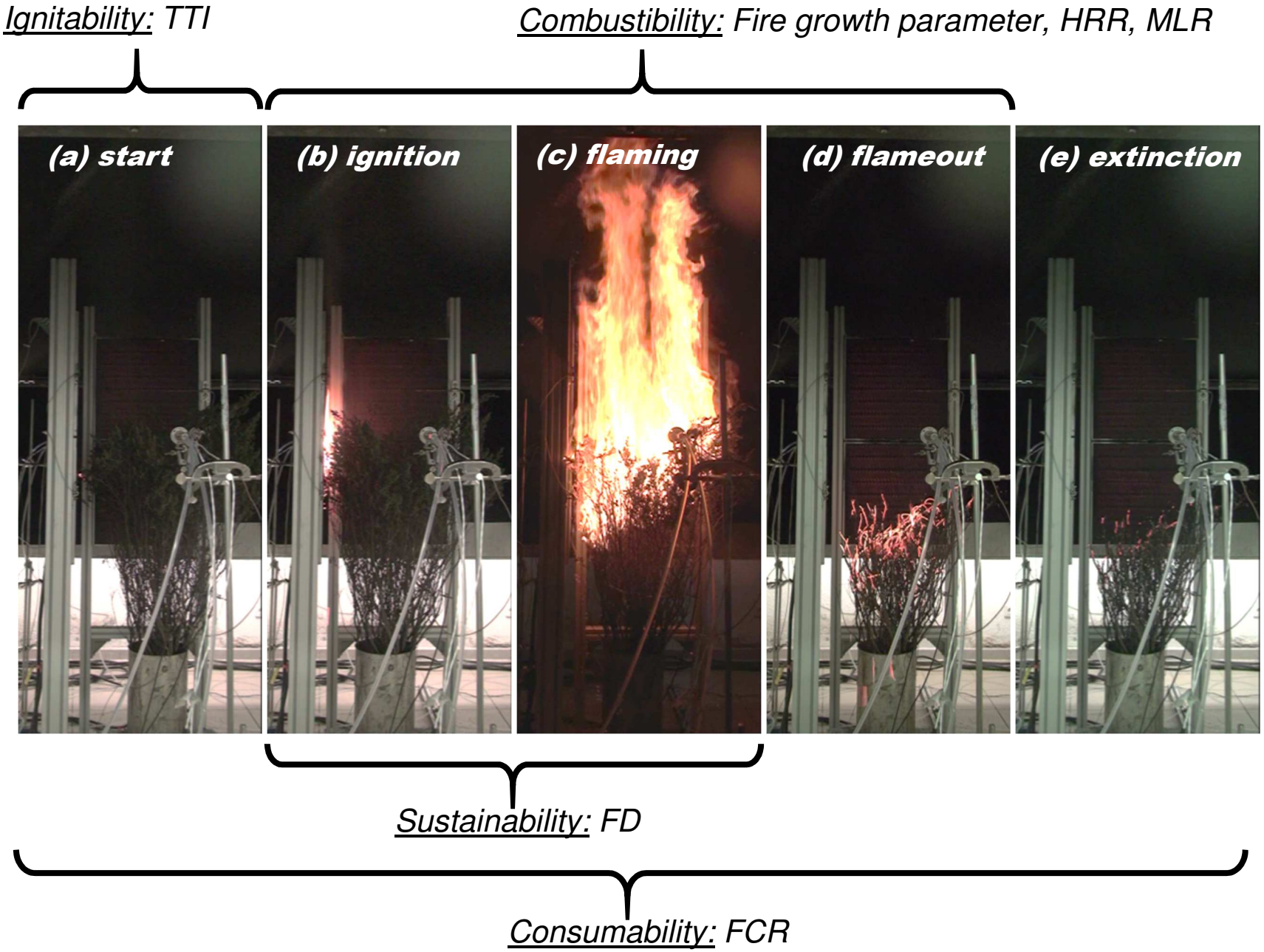

Fig. 3. Measurements of the 4 components of flammability during the different combustion process phases: (a) test start, (b) ignition, (c) flaming, (d) flameout and char oxidation, (e) extinction

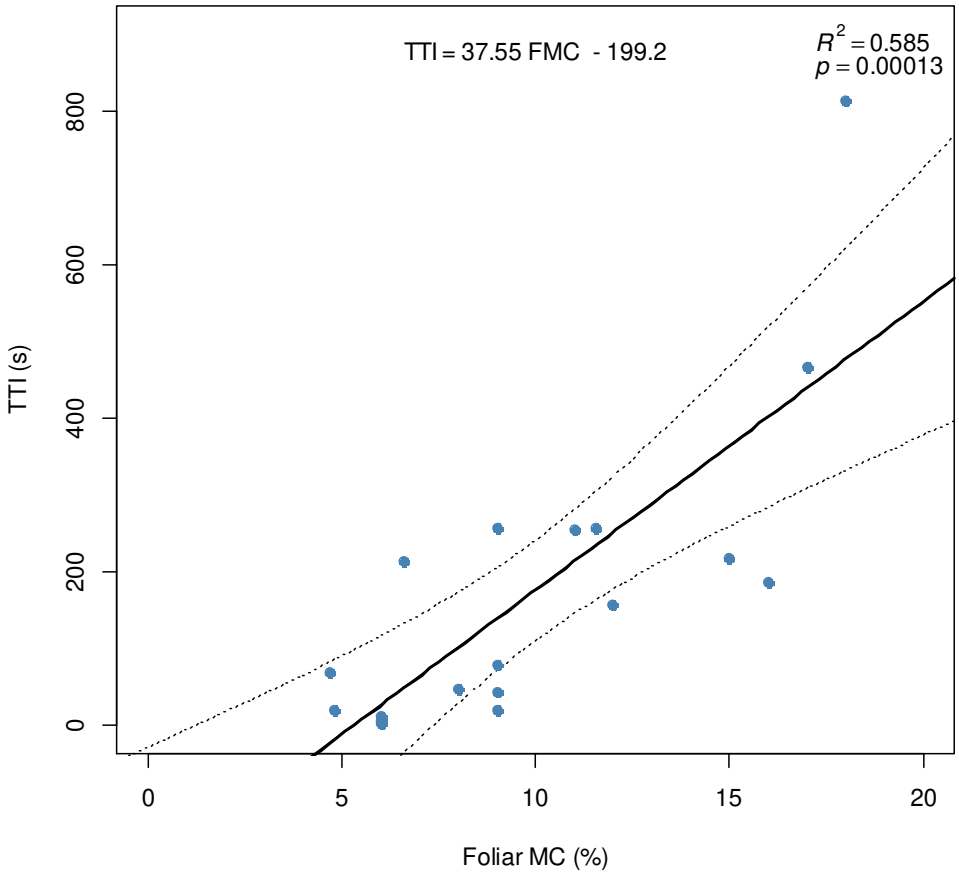

Fig. 4. Influence of foliar MC on ignitability

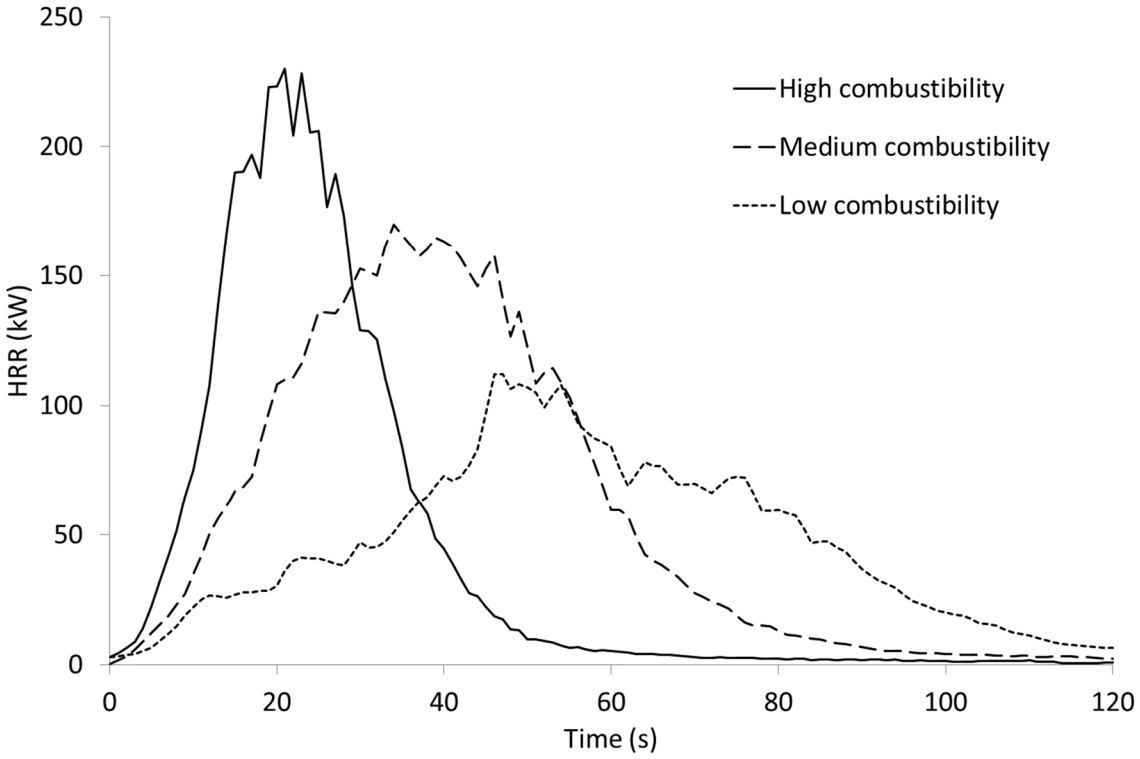

Fig. 5. Examples of HRR after TTI versus time corresponding to low ($\alpha = 0.10$ kW.s^{-2}) medium ($\alpha = 0.22$ kW.s^{-2}) and high combustibility ($\alpha = 0.52$ kW.s^{-2}) for fire tests 4, 14 and 15, respectively

Fig. 6. Fire growth observed 30 s after ignition for different values of α: (a) low combustibility: α = 0.10 kW.s^{-2} (fire test 4); (b) medium combustibility: α = 0.22 kW.s^{-2} (fire test 14) and (c) high combustibility: α = 0.52 kW.s^{-2} (fire test 15)

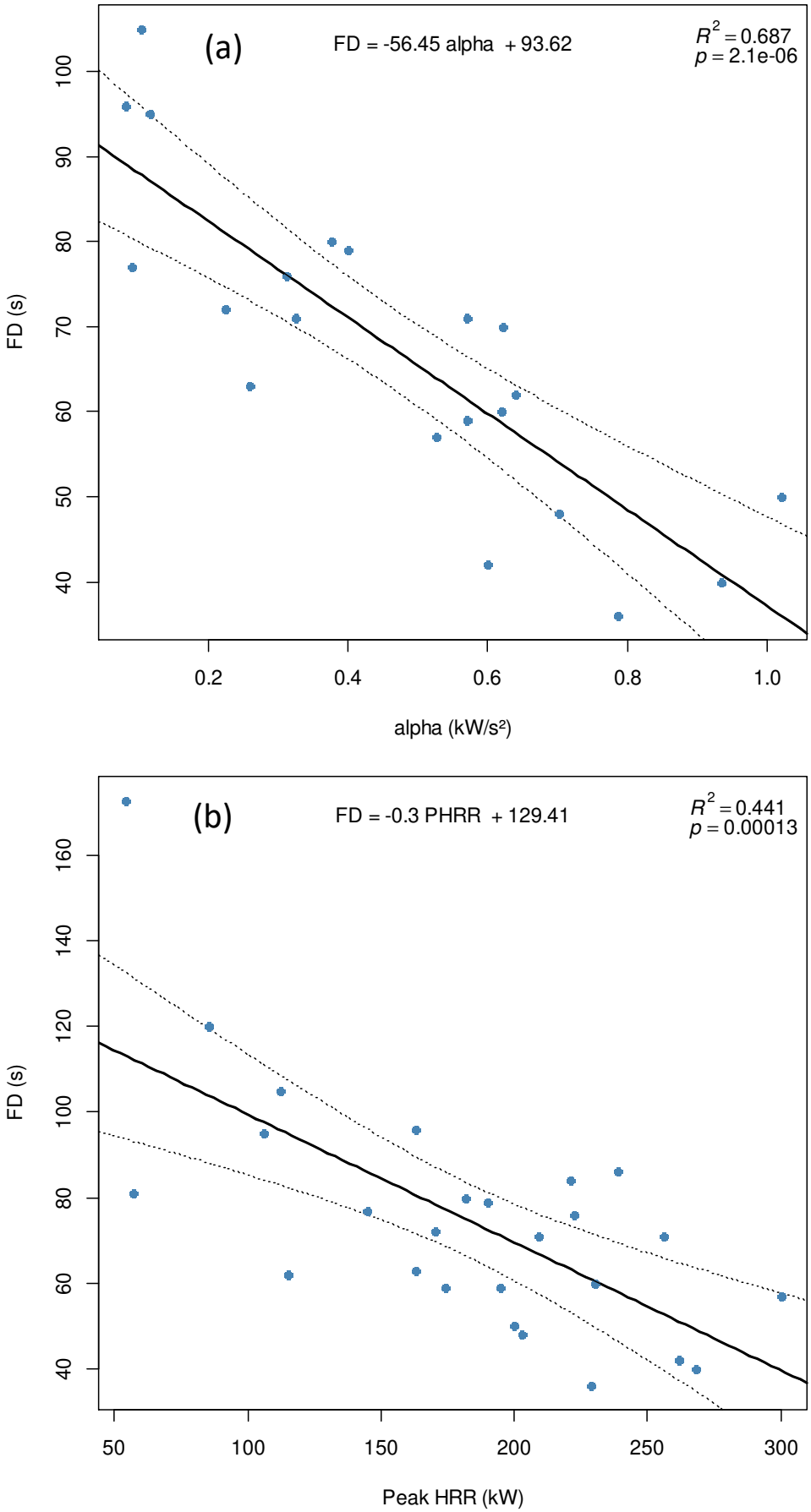

Fig. 7. Relationship between sustainability and combustibility (a) Flame duration FD (s) versus fire growth parameter α (kW.s^{-2}) and (b) Flame duration FD (s) versus peak HRR (kW)

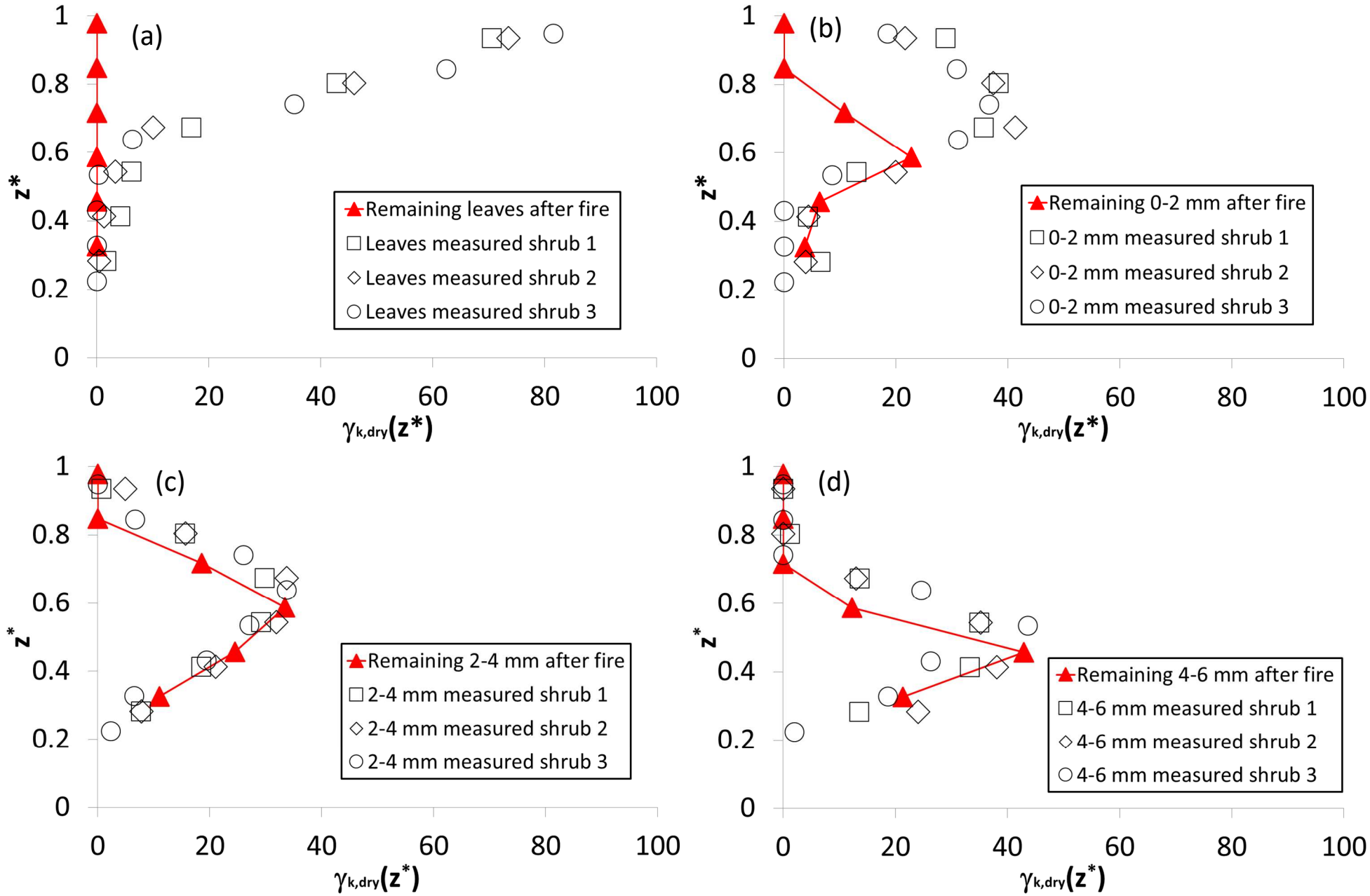

Fig. 8. Characterization of the fuel consumption at particle level: comparison of the mass fraction before (from the destructive measurements of 3 shrub samples) and after the burning (fire test 15), for the different particles size classes: (a) leaves, (b) twigs of 0-2 mm diameter, (c) twigs of 2-4 mm diameter and (d) twigs of 4-6 mm diameter.

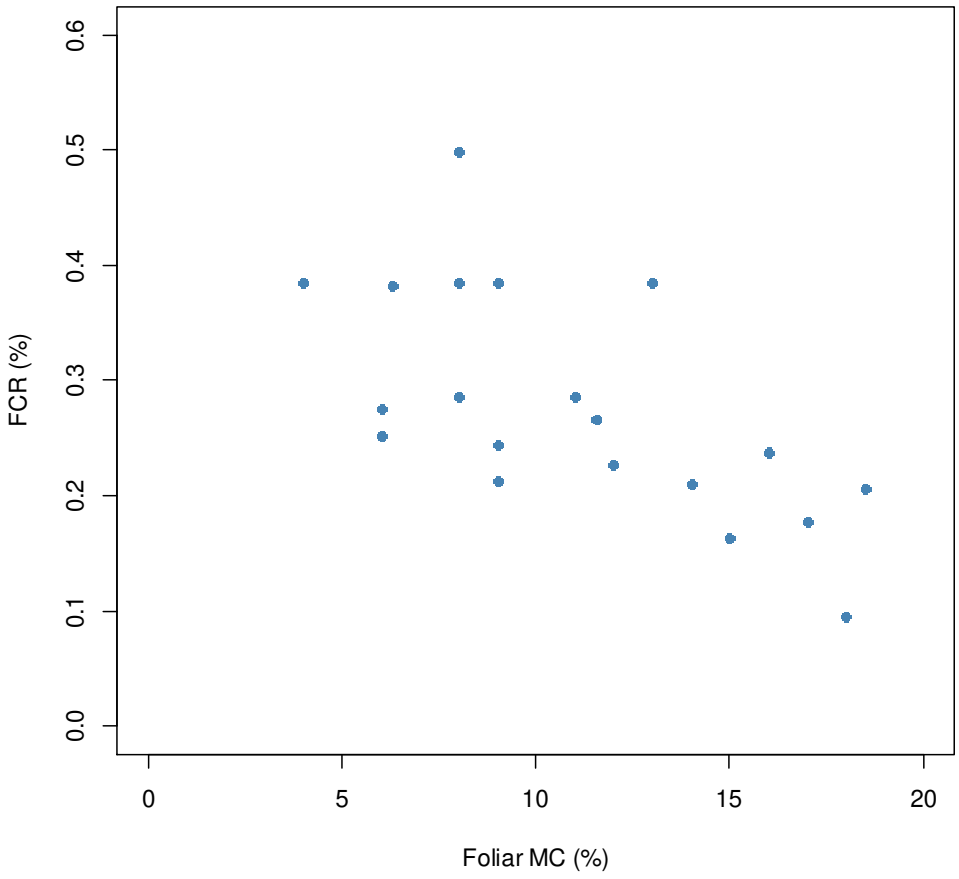

Fig. 9. Fuel consumption ratio versus foliar moisture content

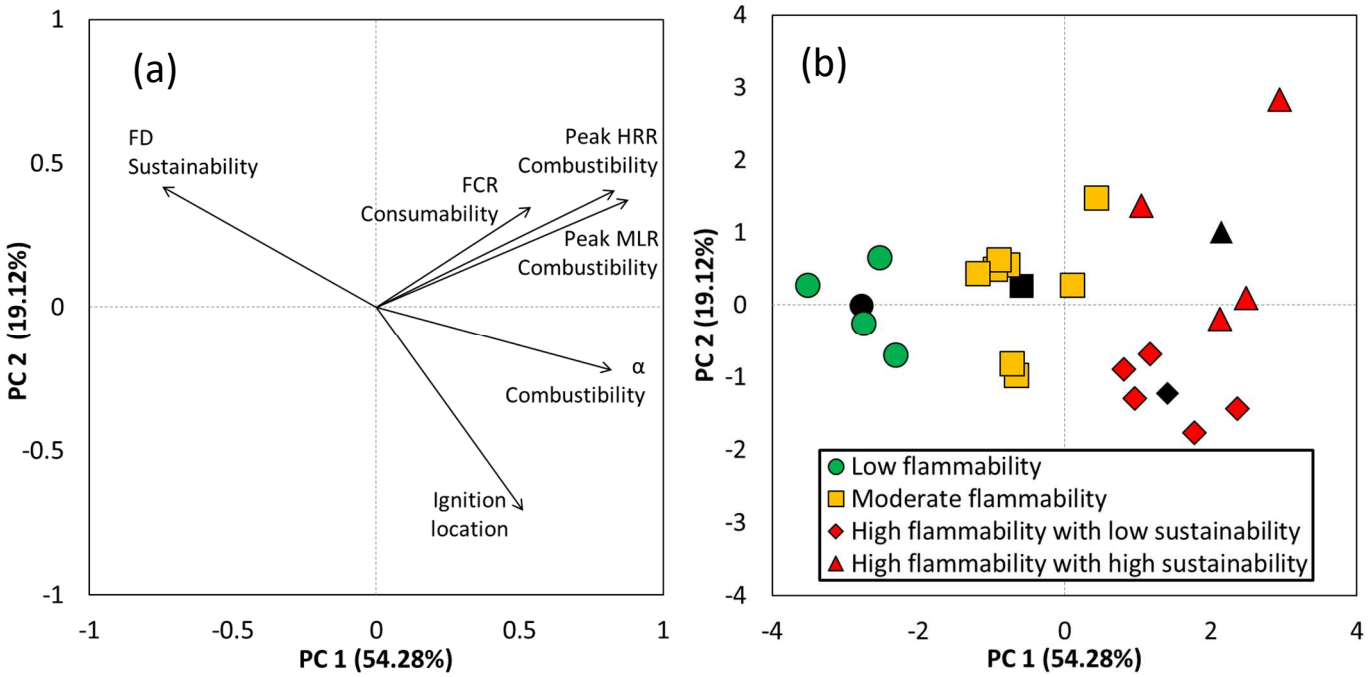

Fig. 10. (a) Principal Component Analysis of flammability variables and (b) Projection of the fire tests on the factorial plane for PC 1 and PC 2 (for each flammability group (circle, square, triangle and diamond), the color and black markers refer to single experiment and barycenter of the corresponding flammability group, respectively)

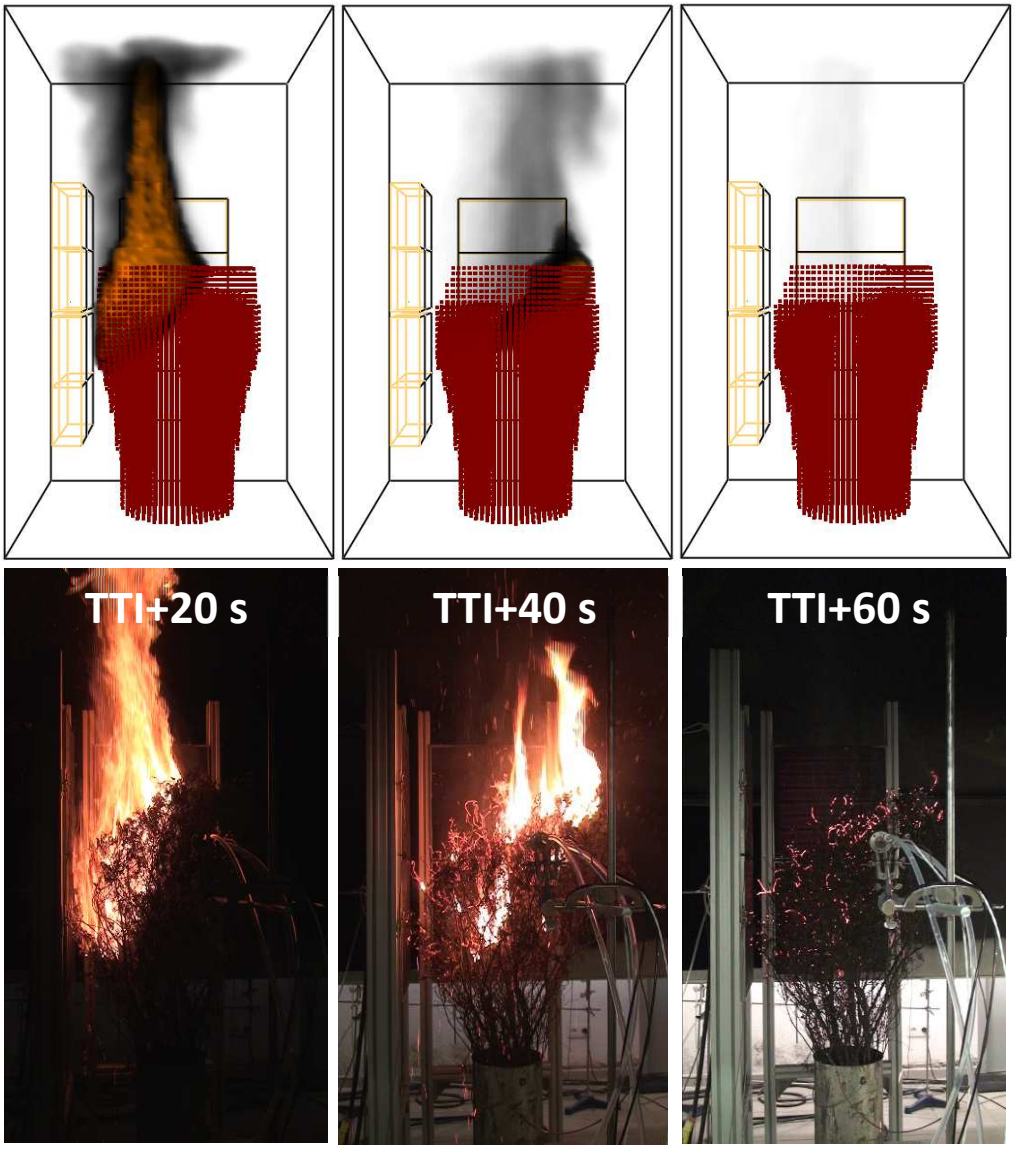

Fig. 11. Comparison of the predicted (200 kW/m^3 isocontour) and observed (test 15) fire spread over time

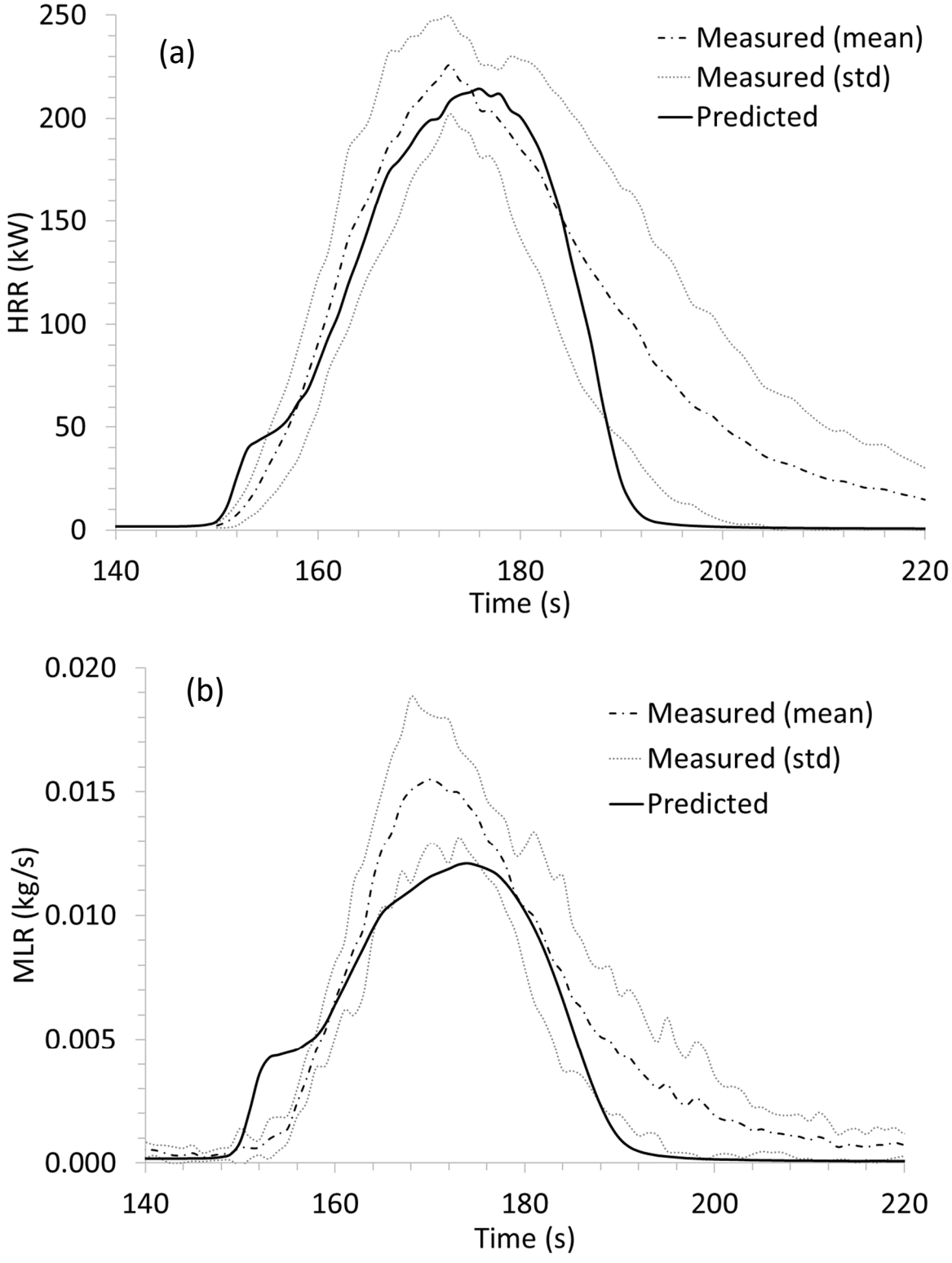

Fig. 12. Comparison of the predictions and measurements (a) HRR and (b) MLR. The experimental data are obtained from the mean (and standard deviation) of 5 fire tests corresponding to the high flammability with low sustainability regime

Large-scale calorimeter

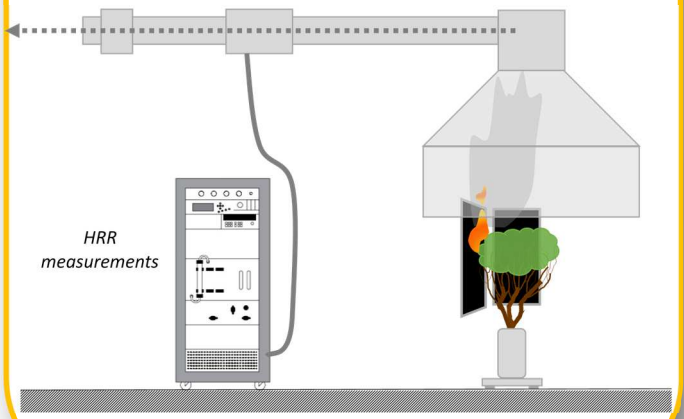

Flammability

Model evalutation

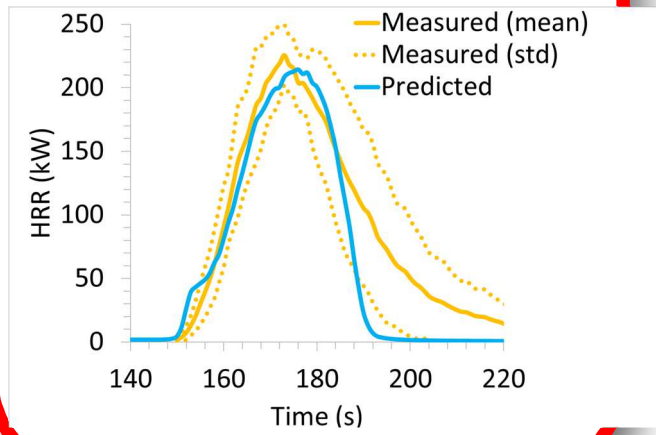

Full-scale plant

Fuel elements characterization

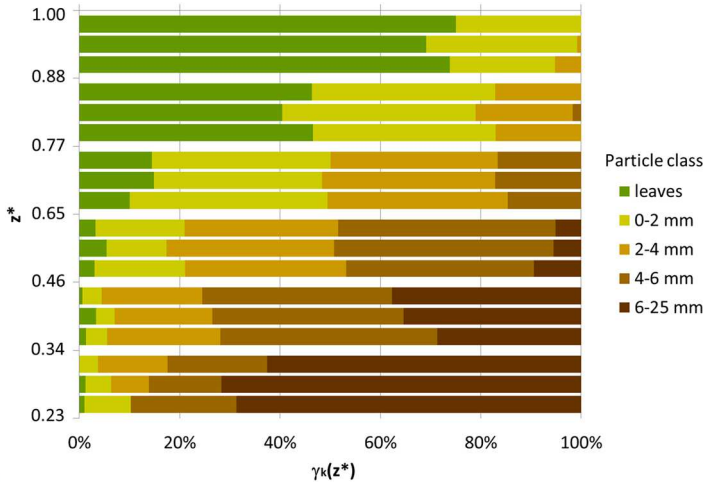

WFDS simulation